LBL-11573 c.2
Preprint

LAWRENCE BERKELEY LABORATORY
UNIVERSITY OF CALIFORNIA

PHYSICS, COMPUTER SCIENCE &
MATHEMATICS DIVISION

Submitted to the Astrophysical Journal

4U1626-67: A PROGRADE SPINNING X-RAY PULSAR IN A 2500 s BINARY SYSTEM

J. Middleditch, K.O. Mason, J.E. Nelson, and N.E. White

September 1980

DISCLAIMER

4U1626-67: A Prograde Spinning X-ray Pulsar in a 2500 s Binary System

J. Middleditch,[1,4] K.O. Mason,[2,4] J.E. Nelson,[1,4] N.E. White[3,4]

ABSTRACT

The binary period of 4U1626-67 has been found from a careful analysis of its optical pusations. A single lower frequency sidelobe of the 2.4% amplitude 7.68s optical pulsations from this X-ray pulsar has been detected on at least 3 different nights in Fourier transforms of high speed photometry obtained with the CTIO 4m telescope. The 0.42% sidelobe pulsations have a frequency which is 0.4011(21) mHz lower than the frequency of the direct pulsations near 130.26 mHz. The weaker sidelobe pulsations are interpreted as arising from X-ray to optical reprocessing on the companion star and are shifted to the lower frequency by the rotation frequency of the binary orbit because the X-ray pulsar spins in the same sense as the orbital motion (direct, or prograde). The orbital period is refined by connecting phases to be either

1. Lawrence Berkeley Lab., University of California, Berkeley
2. Astronomy Dept. and Space Sciences Lab., University of California, Berkeley
3. Goddard Space Flight Center, Greenbelt, MD
4. Visiting Astronomer, Cerro Tololo Interamerican Observatory

This manuscript was printed from originals provided by the author.

2491.06s or 2492.32s ± 0.13s (the epoch for equal phases for the direct and lower sidelobe pulsations is JD 2,444,048,68162). Third harmonic (3F) structure in the lower sidelobe pulsations has enabled us to detect and measure the Doppler phase modulation due to the projected orbital motion and obtain an inclination-independent measurement of the total orbital separation. A simple geometrical model for the optical pulsations from the companion's Roche lobe is developed to calibrate the systematic effects of the measurements of orbital dimensions. With the help of a new limit of $\underline{a}_x \sin i < 0.04$ lt·s established from HEAO-1 data, the corrected values for the orbital parameters are: $\underline{a}_c \sin i = 0.36(10)$ lt·s, $\underline{a}_x + \underline{a}_c = 1.14(40)$ lt·s, $i = 18°^{+18°}_{-\ 7°}$, $M_x + M_c = 1.9^{+2.8}_{-1.4} M_\odot$, $M_x = 1.8^{+2.9}_{-1.3} M_\odot$ and $M_c < 0.5 M_\odot$. The observed lack of amplitude modulation in the companion pulsations synchronous with the orbital period, together with the predictions of the geometrical model allows us to estimate the relative thickness of the disk shadow on the Roche lobe normal to the orbital plane and the radiation law for the non-normal emergence (limb brightening) of the reprocessed optical pulsations from the companion star.

Subject Headings: Stars: variable, X-rays: Binaries

I. INTRODUCTION

The 7 sec pulsar 4U1626-67 is unique among pulsating X-ray sources in being a system with a very high ratio of X-ray to optical emission ($L_x/L_{bol} \sim 600$; Bradt, Doxsey and Jernigan 1979). Because of the absence of background radiation from an early type companion, a relatively large fraction ($\sim 2\%$) of the optical light from the system ($V \sim 18.5$; McClintock et al. 1977) is pulsed at the 7.7 sec period of the X-ray source (Ilovaisky, Motch and Chevalier 1978). A number of authors have searched for evidence of periodic Doppler shifts in the X-ray and optical pulsations that might be caused by orbital motion. The X-ray data have imposed limits on $\underline{a}_x$ sini of 0.1-0.2 light seconds for orbital periods in the range $10^s \lesssim P_{orb} \lesssim 20^d$ (Rappaport et al. 1977; Joss, Avni, and Rappaport 1978; Pravdo et al. 1979; Li et al. 1980). Peterson et al. (1980) have obtained photometry of the optical star which leads them to suspect changes in the phase of the optical pulse. Their data are consistent with an orbital period of less than 7 hours and values of $\underline{a}_{opt}$ sini of $\lesssim 0.5$ lt·s .

In this paper we report the results of high speed photometry of the optical counterpart of 4U1626-67 obtained at CTIO. A number of continuous runs, of duration between six and nine hours, were made with the 4m telescope in order to make a sensitive search for orbitally induced effects in the optical pulsations. Our analysis of the data snows that such effects exist and that the orbital period of the 4U1626-67 system is $\sim$ 40 minutes. In Section II we briefly describe our observing procedures. In Section III

we show how our data can be analyzed to determine the binary period and to provide independent measurements of the total separation, $\underline{a}$, of the binary system and the projected separation of the companion star from the center of mass of the system, $\underline{a}_C$ sini. These two quantities together with limits on $\underline{a}_X$ sini from the X-ray data, yield the orbital inclination and enable the individual masses of the binary components to be determined. In Section IV, the effects of the X-ray shadow cast by an accretion disk on the optical pulsations from the companion star are discussed, while in Section V the origin of the optical pulsations that arise near the X-ray source is considered. Section VI contains a summary of the results and some discussion of possible future observations.

II. OBSERVATIONS

A journal of observations is contained in Table 1. A total of 16 runs were made on 4U1626-67 between April and August 1979; runs 1-5 and 8-13 were made on the 4m telescope, the remainder on the 1.5m telescope. Runs 1-2, 5, 9-10, 11-12, and 13 represent five nights of reasonably long clear observations on the 4m telescope. All observations were made in white light with an EMI 9658R photomultiplier tube with an S20 photocathode (red extended by prismatic reflection), cooled to $\sim -20^{\circ}$. A magnetic collar was used to reduce dark counts to $\sim 20\ s^{-1}$ by reducing the effective photocathode area to a 15mm disk. The typical counting rate from 1626-67 varied from 700 to 1300 counts s^{-1} while the dark sky background through a 6.3" aperture varied from 2000 to 4000 counts s^{-1}. A dead time of 3-5 μsec was used to eliminate afterpulsing (see Middleditch 1976, and Middleditch and Nelson 1976; hereafter MN).

III. ANALYSIS

a. Optical Pulsations from the Companion Star

Figure 1 shows a 6 hour run on 4U1626-67 taken on June 25, 1979, binned at 20s per point. The ubiquitous flaring behavior of amplitude up to 0.2 magnitudes has been noted previously (Middleditch et al. 1979; McClintock et al. 1980).

The data for each run were detrended by the subtraction of a low order polynomial and then Fourier transformed. Power spectra were generated from the Fourier amplitudes and were examined near the 7.68s period where all showed highly significant peaks due to the optical pulsations. The power spectra for the 3 strongest detections of the optical pulsations (all of which have a peak at 130.26 mHz with power in excess of 300 times the local average noise level) are shown in detail in Figure 2. In addition to the main peak at 130.26 mHz (which has been truncated in the Figure) we also find significant power (P) at 129.85 mHz in each of the three runs. No power consistently appears at any other frequency near 130.26 mHz, although other peaks do appear in individual runs, particularly one at 130.56 mHz in run 5. The other two nights of long observations also show peaks of similar relative amplitude consistent with the feature at 129.85 mHz, although with reduced significance due to the lower sensitivity of these runs (the power in the main peak of 130.26 mHz was only $\sim$ 130).

The simplest explanation of the persistent feature of 129.85 mHz is that it is generated by optical pulsations from the non X-ray-emitting companion star produced through the reprocessing of X-ray pulses into optical light (cf. HZ Her, MN 1976)

while the main feature of optical pulsations at 130.26 mHz is produced near or along the line of sight to the X-ray source. The frequency of these 'direct' pulsations was measured by connecting the phases of the 4m runs separately for the April and June data and agrees well with the frequency expected by extrapolation from the X-ray data (Joss et al. 1978; Pravdo et al. 1979) with an uncertainty of 0.01%. The direct optical pulsation frequency also agrees with the ephemeris of Peterson et al. (1980) to within 0.0005%. The frequency of the pulsations reprocessed from the companion is different from that of the direct pulsations because of the orbital motion - the companion "sees" one less or one more (depending on the sense of the pulsar spin) pulse per orbital cylce than an inertial observer. The frequency separation of the direct and companion pulsations averaged over the five strongest runs fixes the orbital period, $P_B(=1/F_B)$, at 2493(15) seconds. The sign of the difference implies the pulsar rotation has the same sense (prograde) as the orbital motion. This is the second measurement of the spin direction of a pulsar with respect to the orbital motion (cf. MN for the first; Her X-1 and Chanan, Nelson and Margon 1978 and Chanan 1978 for the spin of DQ Her wrt the disk's motion about the white dwarf).

No other orbital period (or any other periodic modulation of the direct pulsations at 130.26 mHz) is evident from the data in Figure 2. Modulation periods shorter than 2493s would produce sidelobe(s) farther away from 130.26 mHz than the peaks at 129.86

mHz, would be easily detected by computer analysis while none were detected. Modulation with a longer period (a smaller frequency) than 2493s would produce sidelobe(s) very close to the Fourier peak of the direct pulsations. In order to sensitively search for evidence of such longer period modulation by examining the power spectra in detail near the main pulsations at F_o = 130.26 mHz, the continuous power spectra shown in Figure 2 were constructed using a special Fourier interpolation technique. The technique first established a method for generating the continuous Fourier transform using the interpolation formula:

$$A_r \equiv \sum_{\ell=[r]-m}^{\ell=[r]+m} A_\ell \, e^{-ix} \sin x/x; \; x \equiv \pi \, (r-\ell) \qquad (1)$$

where r is a continuous subscript, the A_ℓ's are the discrete Fourier amplitudes, the brackets denote the nearest integer function and the frequency represented by the ℓth Fourier amplitude is ℓ/T_{FFT} cycles/sec where T_{FFT} is the total time spanned by the Fourier transform. Equation 1 represents a good approximation for a more complicated exact interpolation as long as $N >> m >> 1$, where N is the number of points in the Fourier transform. For our data N is typically 2^{18} while m varies from 50 to 75.

The sidelobes of the main peak (of the form $\sin^2 y/y^2$; $y \equiv \pi(F-F_o)\, T_{run}$) were then removed from the spectrum to clarify its underlying structure (as seen in Fig. 2). This was accomplished by constructing a new discrete lattice of Fourier amplitudes, generated by

interpolation, with a lattice point centered exactly at the main peak and spaced so that the lattice sites correspond with the nodes of the sidelobe pattern of the main peak. The change in the lattice spacing was necessary because $T_{FFT} > T_{run}$ due to the constraint of 2^n points in the FFT and the requirement that the Fourier transform include all of the data (the end sections of such FFT's are padded with the average data value). The continuous power spectra shown in Figure 2 were then generated by equation 1 except that the new lattice point, A_k, under the main peak was set = 0 for all interpolation done outside of $k \pm 1$.

The search for binary or modulation periods longer than 2493s was also negative. Thus, other than the peak at 129.86 mHz we find no persistent single sidelobe at any frequency. Peterson et al. (1980) suggested tentative evidence for a 5 hour period, corresponding to a 0.5 lt·s phase modulation, which would produce two sidelobes centered on the main peak. However, we see no evidence for any observable phase modulation above 0.24 lt·s.

b. The Orbital Phases

We have observed the optical pulsation from the companion star of 4U1626-67 shifted lower than the frequency of the direct optical pulsations at F_o by the amount F_B (the frequency of the binary orbit) due to the sidereal effect of the orbital motion : $F_C = F_o - F_B$.*

*There are in fact some 325 pulsar "days" in each of the system's "years" and thus the sidereal effect is approximately in the same proportion as the Earth's. This is probably the only similarity between 4U1626-67 and our own solar system!

Integrating in time we get $\phi_c(t) = \phi_d(t) - \phi_B(t) + C$, where ϕ_c is the instantaneous phase of the optical pulsation from the companion star, $\phi_d(t)$ is the instantaneous phase of the direct optical pulsations at 130.26 mHz, $\phi_B(t)$, defined as $2\pi(t-t_o)/P_B + \phi_B(t_o)$, is the orbital phase of the system and t_o is the time of the beginning of the run. The constant of integration, C, can be seen to be mainly the phase delay produced by the light travel time across the orbital separation, $\underline{a}$: ie between the X-ray source and the center of pulsed light from the companion star. Then, $\phi_c(t) = \phi_d(t) - \phi_B(t) - 2\pi\underline{a}F_o/c$, where c is the velocity of light. Figure 3 illustrates the orbital geometry.

The equation relating the truly instantaneous phases, $\phi_c(t)$ and $\phi_d(t)$, must also involve a term describing the orbital motion of the companion star around the system center of mass as projected along the line of sight to the observer. Neglecting the similar (but, as we will see, much smaller) modulation term for $\phi_d(t)$, the full equation relating the instantaneous phases is given by:

$$\phi_c(t) = \phi_d(t) - \phi_B(t) - (\underline{a} - \underline{a}_c \sin i \cdot \cos\phi_B(t))F_o/c \text{ (cycles)} \qquad (2)$$

where $\underline{a}_c \sin i$ is the projected distance of the companion star from the center of mass of the system (as seen by an observer at inclination i). The $F_o\underline{a}_c \sin i \cdot \cos\phi_B(t)/c$ term is the phase modulation due to projected orbital motion and will average to zero over several orbital cycles. The orbital phase at which the line of sight from the pulsar to the Earth projects through the

companion star in the orbital plane (superior conjunction of the pulsar wrt the companion) is defined to be $\phi_B = 0$.

This model assumes that the pulse phase of the X-ray beam is a function only of ψ — the azimuthal angle measured in the orbital plane — and does not vary with the polar angle, θ. This assumption is not trivial because the lack of eclipses in the X-ray flux ensures that $\theta(\approx \pi/2) > i$ at the companion star (while $\theta \equiv i$ for the observer and possibly the "direct" pulsations). We have also assumed equal reprocessing times for the direct and companion pulsations. The consequences of a possible deviation from these assumptions are discussed in the end of Section IIId.

When $\phi_c\ (t_o)$ and $\phi_d\ (t_o)$ are measured from the Fourier amplitudes derived from a long time series (i.e. many orbital periods), Equation 2 loses the $\underline{a}_c \sin i$ term and can be regrouped as:

$$\phi_e(t_o) \equiv \phi_d(t_o) - \phi_c(t_o) \approx \phi_B(t_o) + \underline{a}\ F_o/c \text{ (cycles)} \qquad (3)$$

which defines an effective orbital phase, $\phi_e(t_o)$. The last term in Equation 3, $\underline{a}\ F_o/c$, represents the light travel time from the X-ray pulsar to the center of pulsed light on the companion star.

The ϕ_e's in Equation 3 are shown to be compatible with a standard analysis of cycle counting in the Appendix. Times of $\phi_e = 0$ defined near the centers of the runs are used to determine the validity of all trial orbital frequencies which are compatible with the average of the individual F_B measurements obtained from each of the 5 nights. The errors in these times of $\phi_e = 0$ are dominated by the contribution of the less significant lower sidelobe peaks. These

times, their errors, the individual frequencies and the frequency errors are all listed in Table 2.

The cycle counting analysis gave acceptable fits for only two discrete values of the binary period . These are 2492.32s and 2491.05s ± 0.13s which had X^2 values of 1.24 and 3.44 respectively for 3 degrees of freedom. This analysis was shown to pick the same candidate binary frequencies using times of $\phi_e = 0$ defined near the starts of the runs ($t \gtrsim t_o$) which were obtained more directly from the phases of the complex amplitudes of the direct and lower sidelobe Fourier peaks. We hope that the data taken by Peterson et al. (1980) and by Ilovaisky et al. (1980) will ultimately resolve the ambiguity for the orbital period.

Without refering to the complex procedure described in the Appendix, we can easily understand how the distribution of the 5 observations in time severely limits the range of possible periods. In particular, the two measurements in April and the two measurements in June can be obviously connected by 69 and 34 cycles respectively. These two pairs of phase connections separately give periods of 2490.0 ± 3.0s and 2491.3 ± 3.7s which average in a constant manner to 2490.5 ± 2.3s (see Table 2 for the cycle number assignments of the two most likely binary periods).

c. Measuring $a_c \cdot \sin i$

In principle the "direct" pulsations and the lower sidelobe pulsations can be used to measure the orbits of the X-ray source and companion star, respectively, by means of the phase modulation induced by the Doppler effect. This effect would produce sidelobes centered on the frequency of the pulsations in question separated by

units of $1/P_B$ (or F_B = 0.4013 mHz) in the Fourier spectrum. The amplitude of the nth sidelobe relative to the main peak is $J_n(z_\phi)/J_o(z_\phi)$ where J_o and J_n are Bessel functions and $z_\phi = 2\pi F\rho \sin i/c$ is the amplitude of the phase modulation on the frequency, F, due to periodic revolution in a circular orbit of projected radius $\rho \sin i/c$ lt·s (see eg. Abramowitz and Stegun, 1970)

For small z_ϕ, the only measurable sidelobes would be located at $F \pm F_B$. Thus the measurements of the Doppler effects for both the "direct" pulsation at F_o and the companion pulsation at $F_o - F_B$ are complicated because each component of pulsation is superposed on one of the other's two sidelobe frequencies. Furthermore, the measurement of phase modulation for the two components of pulsation at F_o and $F_o - F_B$ using only the single remaining sidelobes at $F_o + F_B$ and $(F_o - F_B) - F_B$, respectively, is susceptable to error due to the possible presence of amplitude modulation with frequency F_B in each component's own pulsation.

In any case, examination of Figure 2 at $F_o + F_B$ reveals a lack of any significant power for all three strong runs which sets an upper limit of 0.20 lt·s for the projected orbital radius of the X-ray source, $a_x \sin i$. Likewise, no amplitude modulation with period P_B can exist in the "direct" pulsations at F_o above a modulation semi-amplitude of 15%.

The measurement of the phase modulation in the lower sidelobe using the Fourier amplitude at $F_o - 2F_B$ is even more difficult because of the smaller amount of power contained in this feature. Moreover, this measurement is contaminated in one case by symmetric sidelobes at $F_o \pm 2F_B$ in Run 9+10 which appear to be consistent with phase

modulation of the "direct" pulsations. The origin of this phase modulation is poorly understood but may be caused by matter with high inclination to the orbital plane.

The Doppler phase modulation becomes easier to detect at higher harmonics if such are present since z_ϕ scales with frequency. Moreover, the cross-contamination due to the two components of pulsation decreases because their separation scales as the degree of the harmonic whereas the sidelobe separation does not. However, the upper limit achieved for the Doppler phase modulation of the direct pulsation at $2F_o$ is no better than that derived near F_o because of the reduced power in the 2nd harmonic.

On the other hand the optical pulsations from the companion were found to contain a much greater relative harmonic structure than the "direct" pulsations, in particular at $3F_o - 3F_B$. Figure 4a shows the continuous power spectrum for Run 5 centered around $3F_o - 3F_B$. Here the harmonic of the companion pulsations at 389.6 mHz has more than double the power from the harmonic of the "direct" pulsations at 390.8 mHz.

Because of the increased sensitivity at this harmonic frequency and the reduced contamination from the 3rd harmonic of the "direct" pulsations we were able to detect and measure the Doppler phase modulation due to the orbital motion of the companion star. Figures 4b and 4c show spectra for the phase and amplitude modulation of the peak at $3F_o - 3F_B$ generated from Run 5 by the following procedure:

Letting ΔF represent the hypothetical modulation frequency, we first find the complex amplitude, a_o, with phase, ϕ_o, at $3F_o - 3F_B$ by continuous interpolation and also generate the

complex amplitudes, a_+, and a_-, at $3F_o - 3F_B \pm \Delta F$. The amplitude of the phase modulation, z_ϕ, can then be measured from the equation:

$$|a_o|\, 2J_1(z_\phi)/J_o(z_\phi)\ .\ e^{i\phi' + i\pi/2} = (a_+ . e^{-i\phi_o} - a_-^* . e^{i\phi_o})\ ;\ i \equiv \sqrt{-1} \quad (4)$$

where the phase modulation is defined by the addition of the term, $z_\phi \cdot \cos(2\pi\Delta F t + \phi')$, to the phase, $6\pi(F_o - F_B)(t - t_o) + \phi_o$, at the 3rd harmonic frequency of the lower sidelobe.

The amplitude modulation at ΔF can also be calculated using the same Fourier amplitudes:

$$|a_o|\ z_A e^{i\phi'} = (a_+ e^{-i\phi_o} + a_-^* . e^{i\phi_o}) \quad (5)$$

where the amplitude modulation is defined by multiplying the periodic signal with the term $(1 + z_A \cdot \cos(2\pi\Delta F t + \phi'))$.

The right hand sides of equations 4 and 5 each represent a direct addition of two statistically well-understood amplitudes. Therefore, the squared moduli of these combinations will each represent twice a quantity which behaves statistically like the power generated from the original Fourier transform. It is these powers of phase and amplitude modulation that are plotted for values of ΔF up to 1.8 mHz (4.5 cycles per 2492s orbit) in Figures 4b and 4c. The phase and amplitude spectra are redundant between positive and negative values of ΔF, but are plotted on both sides of $\Delta F=0$ for purposes of clarity.

The phase modulation plot shows significant power for ΔF of $\pm$ 1 cycle per 2492 second orbit. The figure shows no corresponding amplitude modulation. Other sidelobes near the central peak indicate some modulation on a 10^4 second timescale which is not cleanly resolved into either phase or amplitude modulation. These are well resolved from the orbital modulation sidelobes and cannot affect their

measurement.

The other strong runs (9+10, 11+12) also show the same pattern: phase modulation and no amplitude modulation at the 2492s orbital period in the 3rd harmonic of the lower sidelobe (companion pulsations). The pattern is also measurable in Run 13. The $\sim 10^4$s modulation observed in Run 5 is absent from these runs.

The strength of tnis phase modulation can be directly related to $\underline{a}_c \sin i$ (the projected separation of the companion star from the center of mass of the binary system) through the measurements of $z_\phi = 6\pi(F_o - F_B) \cdot \underline{a}_c \sin i/c$. Individual measurements for $\underline{a}_c \sin i$ were obtained for 4 of the 5 long 4m runs and are listed in Table 3. The mean value for this effective $\underline{a}_c \sin i$ is 0.32 (+0.8, - 0.07) lt·sec. The effective $\underline{a}_c \sin i$ will in general be less than the true $\underline{a}_c \sin i$ due to the difference between the center of the pulsed light for the companion pulsations and the companion's center of mass. The appropriate corrections will be discussed in Section IIIf.

d. The Separation of the Binary Components

The phase of the phase modulation, ϕ', is the orbital phase, ϕ_B, by definition. Thus $\phi_B = 0$ at superior conjunction of the X-ray source with respect to the companion (when the X-ray source is at its greatest distance from the Earth). Five values for ϕ_B measured at the starts of the five runs are listed in Table 3. The true orbital phase, ϕ_B, is related to the effective orbital phase, ϕ_e, derived from the difference between the phase of the direct and lower sidelobe pulsations (Section IIIb), and the light travel time across the system, $\underline{a}/c$, as expressed in equation 3. We can thus combine our measures of ϕ_B and ϕ_e to compute $\underline{a}F_o/c$ directly. The

values of ϕ_e for the beginnings of each runs are also tabulated in Table 3, along with the difference:

$$\phi_e - \phi_B = aF_o/c \qquad (6)$$

The five values derived for a, the effective orbital separation, average to 46.4 ± 15° or 0.99 ± 0.32 lt·s -- a measurement of the total effective separation of the binary system which is independent of the orbital inclination. This is the first instance where the light travel time across a non-solar system binary orbit has been directly measured (cf. Roemer and Scavens, 1676; cf. Gruber, Koo and Middleditch, 1980, for a treatment utilizing the more direct orbital size measurements of visual binaries to check the value of c outside the solar system).

The 90% confidence limits for the fractional semi-amplitude of the 2492s amplitude modulation (z_A) were computed by equation 5 and are listed in Table 3. The limits for all of the runs can be combined to give a 90% confidence upper limit of 0.48 for z_A; i.e. the peak to trough ratio of the companion's pulsed intensity at $3F_o - 3F_B$ must be less than 2.85.

The final entry in Table 3 is ϕ_f, the difference between the values of ϕ_e and ϕ_{e3} defined by:

$$\phi_{e3} \equiv (\phi\,(3F_o) - \phi\,(3F_o - 3F_B))/3;\ \phi_f \equiv \phi_{e3} - \phi_e \qquad (7)$$

The ϕ_f's for the runs are consistent with their average of -22°(7:6). There are at least two possible mechanisms which could plausibly cause a systematic offset of ϕ_{e3} from ϕ_e. The first mechanism is an angular difference between the pulsed radiation pattern as viewed from the Earth and from near the orbital plane. This angular difference, which was assumed to be 0 for equation 2 of Section IIIb, could be due to

a slight obliquity of the pulsar's rotation axis to the orbital plane or to the opacity of columns of accreting matter. A second mechanism may be invoked if the "direct" component of pulsation is really the result of pulsed reprocessing from, for instance, an accretion disk over a wide range of azimuthal angle, ψ (in the orbital plane). In this second case, the loss of amplitude due to geometrical averaging and the resulting phase shifts would be expected to be greater for pulse structure at $3F_o$ than for structure at F_o. The Roche lobe of the companion star would meanwhile more faithfully reproduce the incident equatorial radiation beam pattern in its pulse structure with virtually no geometrical averaging since both its linear dimensions and the azimuthal angle subtended to the X-ray source will be shown to be relatively small.

It is unlikely that differences in reprocessing times between the direct and companion pulsations can contribute to ϕ_f since the latter quantity is defined as the offset of two phase differences and any such effect would contribute equally to both differences and cancel in ϕ_f, provided both reprocessing times are short compared to $1/3F_o$ = 2.56s. Negative values for ϕ_f would be produced only when the reprocessing time for the companion pulsations is greater than the reprocessing time for the direct pulsations and on the order of 2.5s. By referring specifically to the discussion of the reprocessing time, t_c, in MN, the associated pulsed amplitude attenuation, $(1+(\omega_p t_c)^2)^{-\frac{1}{2}}$, and the phase lag, $\tan^{-1}\omega_p t_c$, we can quantify the effects of finite reprocessing time, t_c. A 1.25s reprocessing time, t'_c, for the

companion star and a time, t_c, of 0.25s or less for the direct pulsations would produce the ϕ_f observed, but would also attenuatte the companion pulsations at $3F_o - 3F_B$ by a factor of $\sim$ 2.75 more than the direct harmonic pulsation at $3F_o$. McClintock et al., (1980) estimate that $t_c < 0.5s$ (2σ) for the direct pulsations due to the phase agreement with the simultaneously measured low energy X-ray pulse profile, but the disparity in reprocessing times between the companion and the direct pulsations required to produce ϕ_f seems unlikely unless the third harmonic structure of the companion's pulse is produced by the reprocessing of X-rays with energies in the 3-14 keV range.

We do not know, a priori, whether ϕ_e or ϕ_{e_3} represents the most appropriate measure to use in the analysis of the binary system but we have chosen ϕ_e because of its greater statistical significance and an opinion that the lowermost harmonic components of the pulsation are less than proportionately affected by whatever mechanism is causing ϕ_f to be systematically non-zero.

The spacing between the $3F_o$ and $3F_o - 3F_B$ components of optical pulsation also provides another independent measure of the orbital period, P_B. The spacings for the pairs of peaks for our three strong runs give an average P_B of 2461s but are not consistent with this average. Run 5 gives $P_B = 2487.8s \pm 11s$ while runs 9+10 and 11+12 give 2441s and 2455s respectively. For the latter runs, the harmonics of the "direct" pulsations tend to peak a little higher than $3F_o$ (where F_o is the precisely determined value of the fundamental frequency of the direct pulsation) while the harmonic peaks of the lower sidelobes tend to occur at a lower frequency than $3F_o - 3F_B$. Thus both components

contribute to the effect. By using the value of F_o, precisely determined from the inter-night phasing of the April and June runs, with the $3F_o - 3F_B$ components, P_B was independently determined to be 2476s $\pm$ 8s with all three strong runs now consistent. This value is marginally consistent with the two alternatives near 2492s; some systematic effects from the mechanisms discussed above may be responsible for this (nominally) low value of P_B. No simplification is achieved when P_B is assumed to be less than 2492s since the ϕ_f's do not change. However, even if P_B were not accurately known from the night to night phase assignments the results for $\underline{a}_c \sin i$ and $\underline{a}$ derived above would be affected little, since the procedures used to measure the phase and amplitude modulation defined by Equations 4 and 5 are insensitive to small revisions of P_B or changes in the position of the central peak.

e. Pulse Profiles

Figure 5 shows the pulse profile of the direct pulsations and the companion pulsations for Run 5. The companion pulse profile has been generated by folding along its effective orbit. In addition, corrections have been applied at the fundamental frequency $(F_o - F_B)$ of the companion pulsations to account for the contamination expected from the direct pulsations. The contamination arises from the $e^{-iy} \sin y/y$ sidelobes of the direct pulsations and from the $J_n(z_\phi)$ sidelobes spaced at F_B intervals, one of which includes the peak at F_o, which collapse onto $F_o - F_B$ due to the orbit used to generate the pulse profile. The two profiles differ drastically as suggested by the previously noted difference in harmonic content. The other

strong runs (9+10, 11+12) show a similar difference, although the second highest peak in the companion pulse profile (at phase 1.25) is less distinct.

The apparent relative amplitudes and phases derived from the Fourier amplitudes for the constituent harmonics of the pulse profiles are listed in Table 4. The values from our CTIO runs are reasonably consistent. The agreement with the values used by Peterson et al. (1980) to fit their pulse profiles is not as close,

From the data tabulated in Table 4 it is clear that the major difference between the structure of the companion's pulse and that of the direct pulsation is the relative strength of the third harmonic. This difference increases when the strength of the companion's third harmonic is corrected for the loss of power due to the 0.32 lt-s projected orbit (z_ϕ=0.786, $(J_o(z_\phi))^{-1}$ = 1.17).

No significant structure or peaks other than the previously-discussed integral harmonics of the direct and companion pulsations were present in the pulse profiles and power spectra of any of the runs. In particular, no ½ harmonics were present in the data at a level less than 15% of the direct pulsations (0.36% pulsed fraction) and no additional structure was detected in the two pulse profiles higher than the errors given in Table 4 through the 10th integral harmonic.

f. The Binary Parameters of the 4U1626-67 System

Our detection of the orbital period of 2492 seconds fixes the total mass of the 4U1626-67 binary system at:

$$(M_x+M_c) = 1.29M_\odot(a/1t\cdot s)^3 \qquad (8)$$

To calculate the masses explicitly, it is necessary to know the ratio of the masses and the total separation of the binary system.

In the previous section we have derived the effective orbital separation for the two binary components which is the distance between the centroids of the two pulsed optical light emitting regions. We assume that the centroid of the direct pulsations is located at or near the X-ray source. However pulsations from the companion star would be centered on the face nearest the X-ray source and, therefore, would be offset systematically from the companion's center of mass.

To calibrate the offset of the center of pulsed light from the center of mass of the companion we have performed numerical calculations with the geometrical model described by MN (models 1 and 2). We have assumed that the orbit is circular and the companion star is filling its Roche lobe. This binary system has the shortest known orbital period among X-ray sources, so the assumptions of orbit circularity and corotation for the companion's photosphere are reasonable. The accretion rate implied by the X-ray luminosity of 4U1626-67 further suggests that the companion star is filling its critical Roche potential and funneling material onto the X-ray source through the inner Lagrangian point, L1, via an accretion disk.

Although the accretion stream and the stream-disk intersection feature or "bright spot" expected to be present in this binary system would also be in corotation with the orbital motion and would ordinarily reprocess the X-ray pulses into the lower sidelobe feature, their contribution to the lower sidelobe pulses is likely to be small for two reasons. First, the physical cross-section of the stream

must be on the order of a small parameter, ε, times the physical size of the companion star, where $\varepsilon \sim 0.03$ is the ratio of the kinetic speed of sound in the gas to the orbital velocity (Lubow and Shu, 1975, 1976). Second, the stream is likely to be occulted by the shadow of the accretion disk and thus will not reprocess the X-ray flux. The physical dimension of the "bright spot" normal to the orbital plane will not be much greater than the stream height. Thus the lower sidelobe pulsations are probably due only to pulsed reprocessing in the companion star.

The model used a prograde - spinning pulsar beam which consisted of a pure $3F_o$ profile. The part of the companion's Roche lobe surface visible to the X-ray source and at times to the Earth was divided into $\sim 10^3$ elements with each area element, a_ℓ, reprocessing a pure $3F_o - 3F_B$ pulsation in its own rest frame. A discrete spectrum of Fourier amplitudes, $\{A_j\}$, near $3F_o - 3F_B$ was generated by using the relative phase shifts, $\Delta\phi_{jk} = -2\pi(F_j - (3F_o - 3F_B)) \cdot t_k$ at various sequential times, $t_k \equiv k \cdot \tau$; $k = 0,1023$; $1024\tau = 13/F_B$, and for various sequential frequencies, $F_j \equiv j/(1024 \cdot \tau) \simeq 3F_o - 3F_B$. The phase shifts were applied to the sums of the individual complex amplitudes, $\alpha_\ell \cdot e^{i\phi_{k\ell}}$, corresponding to each area element's pulsations at $3F_o - 3F_B$ with the time-of-light-travel/spin lag phase shifts, $\phi_{k\ell}$, applied. As in MN, $\alpha_\ell = a_\ell \cdot \cos\theta_{k\ell} \cos\psi_\ell \cdot V_{k\ell}/(4\pi r_\ell^2)$, where a_ℓ is the area of the surface element, $\theta_{k\ell}$ is the angle between its normal and the line of sight to the Earth, ψ_ℓ is the corresponding angle to the X-ray pulsar, $V_{k\ell} = 1$ (or 0 if $\cos\theta_{k\ell}$ is negative) and r_ℓ is the distance to the pulsar.

The process of generating the Fourier amplitudes is then

described by the equation:

$$A_j = \sum_{k=0}^{1023} e^{-2\pi i(F_j-(3F_o-3F_B))\cdot(k+\frac{1}{2})\tau} \sum_{\ell} a_\ell e^{i\phi_{k\ell}\cdot\cos\theta_{k\ell}\cos\psi_\ell V_{k\ell}/(4\pi r_\ell^2)} \quad (9)$$

A simplification is achieved (as it was in MN) because $\cos\theta_{k\ell}$ and ϕ_{k_ℓ} are each the sum of a constant and a pure sinusoid of period P_B.

The effective $\underline{a}_c$sini's were calculated as a function of mass ratio by combining the side lobes around the $3F_o - 3F_B$ pulsation component in the same way that these parameters were generated from the actual data. The calculations were performed for an orbital size of 1 lt·s but the results of the model calculations will be insensitive to the exact orbital separation until the size of the visible part of the companion star is on the order of $1/3F_o$(∿2.5 lt·s). The model was also used to predict the strength of the amplitude modulation from the sidelobes at $(3F_o-3F_B)\pm F_B$. A nominal value of 22.5° was taken from the orbital inclination. Three orthogonal views of the companion's Roche geometry used in the calculations are shown in Figure 6. The boundaries of the visibility of the Roche surface at the pulsar and at the Earth for various orbital phases are also plotted.

The first result was obtained using a black body law for the non-normal visibility of the pulsed reprocessing (cos θ; model 1, MN) and a mass ratio of $R = M_c/M_x = 0.1$. The predicted semi-amplitude for the 2492s amplitude modulation was 0.584, exceeding the limit of 0.48 set by the data. The large level of amplitude modulation is due to the changing value of cos θ for the surface elements as the companion's orientation to Earth changes during

its orbit. However, it is realistic to expect that the companion will be partially shadowed by an accretion disc around the X-ray source. In particular, those area elements near the equator which exhibit the greatest changes in cos θ will not be illuminated by the X-ray source. This effect reduces the amount of amplitude modulation expected. However, a calculation using the same parameters as before and including an equatorial disc shadow of 0.05 radians half width reduced the predicted amplitude modulation to 0.48 -- only marginally consistent with the observational data. Although a thicker disc would be expected to reduce the strength of the amplitude modulation further, it would also reduce the total strength of the companion's optical pulsations.

Reducing the orbital inclination substantially below 22.5° would also accomplish a reduction in the amplitude modulation but this would require a bigger and more massive binary system since a lower limit on $\underline{a}_c \sin i$ has already been established. If we take a reasonable limit on the total system mass of 2.5 $M_\odot$ we find that i must be at least 15^0 using the effective value of $\underline{a}_c \sin i$ of 0.32 lt s to establish a further lower limit for $\underline{a}$ in equation 8.

We theretore proceeded with the model without the cos θ factor for the angular pulsed reprocessing law, which is equivalent to the model 2 atmosphere of MN. This model represents an atmosphere which is optically thick to the incident X-rays but which is optically thin to the pulsed visible light. This class of model predicts amplitude modulation stengths which are below the upper limit established by the observed data. It is interesting to note that the model

atmosphere developed by Chester (1977) for HZ Her's pulsations predicts an amplitude modulation of 0.43 when no disk is included. This result is intermediate between models 1 and 2.

Model 2 was used to calculate the systematic correction to the orbital parameters for a variety of mass ratios. The results are tabulated against mass ratio, R, in Table 5. An additional systematic effect was discovered in the model calculations. This effect is thought to be due to the presence of the small but finite amplitude modulation which influences the value of the orbital phase, ϕ_B, measured from the phase modulation in a systematic way. We believe this to be the correct explanation for the observed effect because as the amplitude modulation decreases to zero for smaller values of R, i, or larger disk shadows, this effect also tends towards zero.

To compute a value for $\underline{a}$, the $\phi_{Beff} - \phi_B$ values from Table 5 are added to the $\phi_e - \phi_{Beff}$ value measured from the data to compute an $\underline{a}_{eff} F_o/c$. The $\underline{a}/\underline{a}_{eff}$ correction (which has been calculated from the $3F_o$-$3F_B$ phasing in the model) is then multiplied to yield the final value of $\underline{a}$.

The systematic offset of the apparent orbital phase from the true orbital phase affected the derived value for $\underline{a}$ (and consequently the component masses and inclination) as much as the other systematic corrections whose values were found to be relatively constant over a wide range of models. This is because the orbital separation, $\underline{a}$, is derived from the relatively small phase difference between ϕ_e and ϕ_B, and the systematic offset for ϕ_B varies by up to 20% of that small difference, particularly between models which do and do not include disk shadows.

Since the optical light from the 4U1626-67 system is probably dominated by the disk and since our measurement of the (mostly in phase) pulsed flux from the companion can be used to estimate the solid angle which the disk subtends to the X-ray source (the solid angle subtended by the companion star is known from the mass ratio, R), we can, therefore, estimate the size of the shadow of the accretion disk. We will elaborate on this model in Section IV and estimate a disk shadow half thickness of $\lesssim 0.05$ radians about the equator of the orbital system.

g. The orbital parameters

An examination of the HEAO-1 data of Pravdo et al. (1979) by one of us (N.E.W.) at the 2492s orbital period provides an upper limit to $a_x \sin i$ of 0.04 lt·s (2σ) based on the lack of Doppler phase modulation. This measurement, when combined with the optical pulsation data fixes the mass ratio, R, to be less than 0.1, when the relevant systematic corrections are applied from Table 5. The corrected value for $a_c \sin i$ is:

$$a_c \sin i = 0.36 \pm 0.10 \text{ lt·sec} \tag{10}$$

Similarly, the corrected value for the total orbital separation, a, is:

$$a = 1.14 \pm 0.40 \text{ lt·s} \tag{11}$$

These two results combine to set the limits on i:

$$i = 18^\circ \, {}^{+18^\circ}_{-\ 7^\circ} \tag{12}$$

while the total mass of the system from equation 8 is set at:

$$M_x + M_c = 1.9^{+2.8}_{-1.4} M_\odot \tag{13}$$

and the individual masses are:

$$M_x = 1.8^{+2.9}_{-1.3} M_\odot$$

$$M_c < 0.5\ M_\odot \qquad (14)$$

We note that the uncertainties in equations 12, 13 and 14 are correlated so that the limit on the mass ratio, R, is not violated.

If we further assume a mass-radius relation for the companion star filling its Roche Lobe, we can place additional constraints on the masses (cf. Li et al. 1980). If the companion is a main sequence dwarf, M_c must be 0.08 $M_\odot$, and M_x is greater than 0.8 $M_\odot$. In comparison, if the companion is a white dwarf its mass is 0.02 $M_\odot$ and the minimum orbital size implies that the X-ray source mass is greater than 0.50 $M_\odot$.

Because of the rate at which the X-ray pulsar is spinning up (e.g. Joss et al. 1978) and the observed luminosity of the X-ray source, it is probably a neutron star. If the mass of the neutron star is 1.4 $M_\odot$ and has a 0.02 $M_\odot$ white dwarf or a 0.08 $M_\odot$ main sequence dwarf as its orbital companion, then the mass ratio of the system is 0.014 or 0.057 respectively and the corresponding values of $a_x \sin i$ are 0.006 and 0.023 lt·s. Further X-ray observations may conclusively eliminate a main sequence dwarf as the companion to the X-ray source.

It is interesting to note that the mean density of the companion star is of order 200 gm cm^{-3} for any orbital size or mass ratio because the masses scale as the cube of the orbital size and the limiting dimensions of a Roche lobe scale as the cube root of the mass ratio (see,e.g., Chanan, Middleditch and Nelson, 1976).

h. The 1000s Flaring

The ubiquitous 25-50% variability which is present in the 4U1626-67 system appears in Figure 1 (and all of the data) to be

10^3s flares occuring every $3 \cdot 10^3$s (as opposed to $2 \cdot 10^3$s long absorption dips). The flares have been examined using the auto-correlation function and the low frequency region of the Fourier transform for Runs 5 and 10 -- the two longest un-interrupted segments of the data. Long term trends due to background and transparency changes were removed from the runs by subtraction of cubic polynomials. The power in the low frequency regions of Runs 5 and 10 shows non-monotonic behavior with frequency, similar to that described in Li et al., (1980), but again no simple period could be derived from the pattern. The autocorrelation function for Run 10 displays a peak of 15-20% correlation at 1050s delay and another of 10-15% correlation at 2100s delay with zero correlation near 500-600s and a negative 15% correlation at 1600s. The pattern for Run 5 was similar, though not as distinct.

The amplitude of the direct pulsations in Runs 5 and 10 was measured for 128 time sub-intervals and then cross-correlated with the total optical intensities for the same sub-intervals to test the direct pulsations for variations congruent to the flickering in the respective runs. Positive correlations of 70(35)% and 35(30)% were obtained for the runs at zero delay, with Run 10 peaking at over 50% correlation, when the pulsation amplitude fluctuations preceded the flaring by $\sim$ 270s. A cross correlation result of 100% would imply that the amplitude of the direct pulsations have the same relative variation as the intensity of the star. Any non-4U1626-67 variations remaining in the time streams due to imperfect match-ups between the real background variations and the cubic polynomials

subtracted would cause the cross correlation analysis to underestimate the degree of correlation. The cross correlation function varied from + to - on a 10^3s scale of delay change as would be expected by the 10^3s timescale of the flickering. The errors quoted are the expected RMS values for the excursions of the correlation function over this timescale. The variations expected and observed in the correlation function on timescales shorter than 10^3s are smaller. Thus

there is evidence that the direct optical pulsations in 4U1626-67 are subject to at least part of the flickering experienced by the total intensity.

The effect of the flickering amplitude modulation sidelobes of the direct pulsations on the noise level of the the power spectrum near F_o can be shown to be negligible. The low frequency region of the power spectra for Runs 5 and 10 indicate that the flickering produces about 3% semi-amplitude of modulation in each Fourier resolution element. If we use Equation 5 with $z_A = 0.03$ and $a_o \sim \sqrt{350}$ for the direct pulsations, then the contribution to a_+ and a_- is only 0.28, adding less than 10% to the average noise level of the power spectrum.

However, the direct effect of the flaring or flickering on the power spectra of the runs extended well beyond 1 mHz. The noise level at 130 mHz in the power spectra for Runs 9+10 and 11+12 was 2.25 times that expected from Poisson statistics for data count rates averaging 2700 s^{-1}(ie 2.7 times the 10^3 s^{-1} count rate from 4U1626-67 alone). Equivalently, the flickering of the star contributes as much noise power at 130 mHz as a statistical source at 17.3 magnitudes. The mean semi-amplitude of the flickering at 130

mHz is 0.1% of the total light from the star. An attempt to reduce the effect of the flickering at 130 mHz by detrending the Run 9+10 data stream using a running quadratic fit spanning 125 seconds of time had absolutely no effect on the power above 0.02 Hz. The variance of the data as indicated by the power spectrum leveled off to the Poissonian value by the frequency of the third harmonic, 390 mHz.

IV. THE SIZE OF THE DISK SHADOW

The observed strength of the companion's pulsations can be linked to the thickness of the accretion disk and the effective pulsed fraction of the X-ray beam near the orbital plane by a simple geometrical treatment of the energy balance in 4U1626-67. We assume that the X-ray heating of the gas in the binary system dominates the intrinsic luminosity of the companion star as well as the luminosity that the disk generates from the transfer of its material to lower gravitational potentials. We also assume that the optical luminosity of the X-ray source is small compared to the disk's luminosity from the reprocessing of X-rays.

The luminosity of the disk is assumed to be proportional to the solid angle, Ω_{disk}, which it subtends to the X-ray source:

$$L_{disk}^{DC} = (\Omega_{disk}/4\pi).L_x.\gamma \qquad (15)$$

Where γ is the efficiency of the reprocessing of the X-ray flux into visible light and L_x is the X-ray luminosity. The γ factor is probably small for 4U1626-67 for two reasons: First, most of the hard X-rays in the spectrum which Compton scatter in the disk before photoionizing will escape from the disk in the direction normal to the plane of the disk. Second, most of the energy from the X-rays that are reprocessed

goes into the UV flux rather than the visible. The very negative U-B value of this system (-1, McClintock et al. 1977) supports a large value for the bolometric correction. A γ of about 0.01 and an $\Omega_{disk}/4\pi$ of about 0.02 could account for the observed L_x/L_v of $\sim$5000 (the L_x/L_{bol} is $\sim$ 600, Bradt, Doxsey and Jernigan, 1979).

The time averaged luminosity of the companion star, L_c^{DC}, would similarly be proportional to $\Omega_{RL}/4\pi \cdot L_x \cdot \gamma$ where Ω_{RL} is the solid angle subtended by the unshadowed part of the Roche Lobe filling companion. We expect that the L_c^{DC} will be modulated at some level with the orbital period, P_B, due to the changing aspect of the Roche surface. No binary light curve was apparent when the data were folded at the orbital period, but we can set a limit of only 5% to the semi-amplitude of the modulation because of the flickering in the system. The actual semi-amplitude of this modulation is expected to be much lower than this limit because of the low orbital inclination of the binary system. Thus there is no way to estimate L_c^{DC} using these data.

We are therefore forced to consider only the pulsing light from the companion star:

$$L_c^{AC} = (\Omega_{RL}/4\pi) \cdot L_x \cdot \gamma' \cdot pf_x \cdot (1+(\omega_p t_c')^2)^{-\frac{1}{2}} \qquad (16)$$

where pf_x is the effective X-ray pulsed fraction, γ' is the reprocessing efficiency for the X-ray flux incident on the surface of the companion star, $\omega_p = 2\pi F_o$ and t_c' is the reprocessing time for the X-rays in the companion's atmosphere. The bolometric correction factors in γ' and γ cannot differ by much since the material in both the companion and the disk is reprocessing the same incident X-ray spectrum. Furthermore, although the net Compton reprocessing efficiency of the companion will be more than that of the disk, the ultimate re-

processing of these "extra" hard X-rays that are not lost to Compton scattering will not contribute much to the pulsed reprocessing, since it will occur with a reprocessing time which will be on the order of the pulse period (∿10s, see, e.g. Chester, 1979). There is evidence from the study of the colors of the pulsed reprocessing in HZ Her at 1.24s (Nelson, Chanan and Middleditch, 1977; Chanan, 1978), in DQ Her at 71s (Chanan, Nelson and Margon, 1978) and in WZ Sge at 28s (Middleditch, Nelson and Chanan, 1978) that the difference in the spectra of steady reprocessing in the disk and pulsed reprocessing in the companion is not great. We therefore conclude that γ' and γ are likely to be equal to within factors on the order of unity.

Equations 15 and 16 may be combined together using the corollary from the above discussion that:

$$L_c^{DC} = (\Omega_{RL}/4\pi) \cdot L_x \cdot \gamma \qquad (17)$$

to give,

$$(1+(\omega_p t_c)^2)^{-\frac{1}{2}} (L_c^{AC} / (L_{disk}^{DC} + L_c^{DC})) \cdot ((\Omega_{RL}+\Omega_{disk})/\Omega_{RL}) = pf_x \qquad (18)$$

For low inclination, i, the fluxes observed for L_c^{AC}, L_c^{DC} and L_{disk}^{DC} will result from the visibility of approximately ½ of the total radiating surface in each case. Thus the left side of equation 18 can be directly simplified:

$$(1+(\omega_p t_c)^2)^{\frac{1}{2}} \cdot pf_c \cdot ((\Omega_{RL}+\Omega_{disk})/\Omega_{RL}) = pf_x, \text{ or:}$$
$$\Omega_{disk} = \Omega_{RL} \cdot (pf_x/pf_c(1+(\omega_p t_c)^2)^{-\frac{1}{2}} - 1) \qquad (19)$$

where pf_c is the pulsed fraction of the companion pulsations wrt the total optical light from the 4U1626-67 binary system, nominally 0.0042. The apparent solid angles for the companion's Roche lobe in Equation 19 were calculated using the geometrical model. A correction of 14 to 17% for R = 0.1 should be applied to the model pulsed fractions at $3F_o - 3F_B$ to predict the pulsed fraction at

F_o-F_B. The need for the correction occurs because spin phase interference across the Roche lobe reduces the pulse amplitude more at $3F_o$-$3F_B$ than at F_o-F_B. The numbers in parenthesis in column 5 of Table are those which have been generated by models at $F_o - F_B$ to calibrate this effect. The minimum pf_x values listed in the last column of Table 5 were calculated without using this correction since it tends to unity as the Roche Lobe size is diminished for values of $R < 0.1$ and for finite disk shadows. The only other parameter which should properly be calculated at $F_o - F_B$, the phase lag due to $\pm a_{effective}$, changed by less than 1% between the models calculated at $3F_o - 3F_B$ and those calculated at $F_o - F_B$.

An upper limit for the disk shadow thickness may be estimated at $\pm$ 0.075 radians or $\pm$ 4.°3 using the Model 2 atmosphere, a 15% pulsed fraction for the low energy X-rays established by Rappaport et al. (1977) (cf. also Pravdo et al., 1979), $t_c' = 0$ and a mass ratio of 0.1. The upper limit reduces to an estimated value for the disk shadow size when the following factors are included in the model:

1. If part of the disk is optically thin as seen from Earth the light from both the upper and lower halves of that part contribute to the total optical luminosity.
2. The intrinsic optical luminosities of the disk, X-ray source and the companion star.
3. A finite reprocessing time, t_c', for the X-rays in the atmosphere of the companion.
4. Pulse cancellation by the reprocessing of medium energy X-rays in the companion star.
5. The possibility that $pf_x < 0.15$ or the mass ratio, $R < 0.1$

Only a higher X-ray pulsed fraction, "in phase" reprocessing of the

medium energy X-rays, an R > 0.1 or a Model 1 atmosphere will increase the required disk thickness. However, the Model 1 atmosphere is likely to require a larger t_c' than the Model 2 atmosphere. When all the factors are considered, a disk shadow thickness greater than $\pm$ 0.05 radians is unlikely. The probable value for the disk shadow thickness reduces to $\pm$ 0.02 radians for R = 0.01. Now that we have established the size of the companion's Roche Lobe relative to the disk thickness, the mass ratio, R, can be determined via the disk thickness by using the observed $L_x/L_v \sim 5000$ and by modelling the X-ray to optical reprocessing efficiency in the disk.

V. THE ORIGIN OF THE DIRECT PULSATIONS

The similarity between the shape of the direct optical pulsations and the low energy X-ray pulse profile has been noted previously (McClintock et al. 1980, Peterson et al. 1980). If the region that gives rise to the direct optical pulsations is illuminated by X-rays with a pulsed fraction of 15% (Rappaport et al., 1977; Pravdo et al., 1979) then the geometrical efficiency of the reprocessing region can be no worse than pf_{direct}/pf_x = 0.024/0.15 = 0.16, where pf_{direct} is the pulsed fraction of the direct optical pulsations. Similarly, if the direct pulsations originate from the immediate vicinity of the X-ray source, then the value of pf_{direct}/pf_x suggests that at least 16% of the total optical luminosity originates from this region.

There is no clear indication of where the direct pulsations originate. One possible location where X-ray reprocessing may give rise to optical pulsations is the accretion disk that feeds the X-ray source (see, e.g. McClintock et al. 1980). However, the reprocessing of a non-collimated or coplanar X-ray beam in a symmetric disk would be expected to produce optical pulsations inefficiently at the low

orbital inclination of 4U1626-67, because the azimuthal symmetry is preserved. The X-ray beam cannot be sufficiently collimated and non-coincident with the plane of the orbit to affect the azimuthal symmetry of the disk illumination, since there is no periodic amplitude modulation in the companion pulsations.

If the direct pulsations nevertheless originiate in the disk, then the similarity between their shape and that of the low energy X-ray pulse must be coincidential. The profile of the X-ray beam in the orbital plane (and the plane of the accretion disk) must be more or less faithfully reproduced by the optical pulsations from the companion, because of its small size and the small azimuthal angle subtended by this star at the X-ray source. The profile of the direct optical pulsations would thus be produced by the geometrical averaging, over the different parts of the disk, of the complex X-ray pulse profile that is indicated by the companion pulse. A difficulty may arise in this interpretation since the relative strengths of the fundamental and 2nd harmonic components is the same for the direct and companion pulsations (although the phases differ), whereas the relative strengths of the two 3rd harmonics differ by almost an order of magnitude (cf. Table 4). Production of the third harmonic of the companion pulsation via hard X-ray reprocessing might eliminate this difficulty. A further constraint on disk models for the direct pulsations is their phasing with respect to the X-ray pulses. McClintock et al. (1980) have shown that the low energy X-ray and direct optical pulsations are in phase to within 0.5s. In the context of a disk reprocessing model, this implies that the direct optical pulsations are effectively produced on the side of the

accretion disk nearest the Earth. We note that this phasing is implicitly assumed in Equation 2 and is verified by our measurements of $\underline{a}F_o/c$ which average to $+46^o$ rather than -134^o, as would be the case if, for instance, the direct pulsations appeared to originate from the disk's far side (as they do in DQ Her, for example; Chanan, Nelson and Margon, 1978).

VI. SUMMARY AND CONCLUSIONS

a. The Orbital Period and the Pulsar Spin

Our optical observations of 4U1626-67 have revealed a weak component of pulsation (0.42%) at a frequency which is 0.4 mHz lower than the 2.4% optical pulsations at the nominal X-ray pulse frequency. The weak component of pulsation almost certainly originates from pulsed X-ray reprocessing from the atmosphere of a star which is the binary companion of the X-ray source. The frequency of the companion pulsations has been shifted with respect to the direct pulsation frequency by the sidereal effect of the orbital motion. The orbital period was thus estimated to be near 2493s using the average separation of the two optical pulsation components. The sign of the frequency shift of the sidereal effect for the companion pulsations (to a lower frequency) requires that the X-ray pulsar spins in the same sense as the orbital motion.

The differences of the phases of the two components of pulsation derived from the Fourier transforms of long time series were used to define a set $\{\phi_e\}$ representing measurements of the orbital phase, ϕ_B, plus a constant offset due to the light

travel time across the orbit, $\underline{a}F_o/c$. Only two discrete values for the orbital period, P_B, were consistent with the P_B derived from the average of the individual measurements and with the absolute cycle numbers assigned to the ϕ_e's by the discrete value of P_B. These two periods are 2491.06s and 2492.32s $\pm$ 0.13s. Further observations are needed to resolve this ambiguity.

b. The Dimensions of the Orbit

The discovery of structure in the lower sidelobe at its 3rd harmonic frequency makes possible the measurement of the Doppler phase modulation due to the orbital motion of the companion star. The amplitude of this modulation measures the projected orbital radius of the companion star. The phase of the Doppler phase modulation is the orbital phase, ϕ_B, by definition. The light travel time across the orbit, $\underline{a}/c$, was then derived from the $\phi_e - \phi_B$ values for five runs giving an inclination-independent measure the size of the orbital system. No amplitude modulation was detected at the orbital period in the companion's $3F_o - 3F_B$ pulsing component above a modulation semi-amplitude of 0.48 (90%). In addition, the existence of the $3F_o - 3F_B$ component and the sidelobes of its Doppler phase modulation at $3F_o - 3F_B \pm F_B$ provided two more independent measures of the orbital period of the binary confirming the value obtained from the F_o and $F_o - F_B$ components.

A geometrical model for the companion's pulsations was used to calibrate the systematic effects due to the finite size of the companion's Roche lobe wrt the orbital separation. The model produced too much amplitude modulation when a black body law (cos θ) was used to predict the strength of the pulsed reprocessing for a non-zero

angle of emergence, θ, unless $\sim$ 20% of the Roche lobe surface was shadowed by an equatorial disk around the X-ray source. Calculations performed without the cos θ factor (Model 2) were found to agree with the amplitude limit in all cases.

The observed pulsed fraction of the companion pulsations was used in a simple model to constrain the thickness of the equatorial X-ray shadow of the disk on the companion's photosphere. If the low energy X-ray pulsed fraction in the orbital plane is the same as that observed from the Earth (0.15) then the disk shadow thickness can be no greater than $\pm$ 0.05 radians or $\pm$ 2.8°. Values for the disk shadow thickness between $\pm$ 0.05 and $\pm$ 0.02 radians were used with the mass ratios, R, ranging from 0.05 to 0.01 to establish the values of the 4U1626-67 orbital parameters, corrected for systematic effects:

	Model 2	Model 1
$\underline{a}_c \sin i$	= 0.36(10) lt·s	0.38(10) lt·s
$\underline{a}_c + \underline{a}_x$	=1.14(40) lt·s	1.02(40) lt·s
i	= $18^{\circ}(^{+18}_{-7})$	18° (7)
$M_x + M_c$	= $1.9(^{+2.8}_{-1.4})\cdot M_{\odot}$	$1.4(^{+1.4}_{-1.1})\ M_{\odot}$
M_x	= $1.8(^{+2.9}_{-1.3})\ M_{\odot}$	$1.3(^{+1.5}_{-1.1})\ M_{\odot}$
M_c	< 0.5 $M_{\odot}$	< 0.3 $M_{\odot}$

The higher values of the inclination for Model 1 have been eliminated by requiring the model amplitude modulation to be less than the observed limit of 0.48. Improved limits or measurements of the level of amplitude modulation of the $3F_o$ - $3F_B$ component at the orbital

period will help to completely eliminate model 1 as a viable alternative. The negative values for ϕ_f (measured between the third harmonic phases and the fundamental phases) may also indicate that the ϕ_e values contain hidden systematics that affect the value of the orbital separation and consequently, the stellar masses. One example of such a possible systematic effect is an obliquity of the pulsar's axis of rotation wr.t. the orbital plane. Finally, if the direct pulsations originate from the near side of a symmetric disk, the values for $\underline{a}F_o/c$ must be corrected by adding $r_d F_o/c.(1-\sin i)$, where r_d is the distance from the X-ray source to the center of pulsed light from the disk.

c. Possible Further Study of the 4U1626-67 System

Since it is unlikely that the 10^3s flickering will ever be understood on any basis other than a completely stochastic one, it is unlikely that small light deviations associated with the orbital motion will ever be detectable unless the flickering goes away. Therefore, the method of measuring the orbital phases using ϕ_e presented in this paper represents the only way of studying the long time evolution of the 4U1626-67 binary system. The orbital period of this binary can be expected to show a large rate of change with time because of the high angular momentum transfer rate implied by the steady pulsar spin up (Joss et al. 1978; Peterson et al. 1980). Assuming that the mass transfer process carries angular momentum from the companion to the pulsar (see, e.g., Pringle, 1975) we expect values of $\dot{P}_B/P_B$ of 2.10^{-8} to 2.10^{-7} yr^{-1} depending on the distance of the source (4 - 12 kpc, Joss et al. 1978). These rates would produce a measurable secular orbital phase gain of 0.1 cycles

in 9 and 28 years respectively. In constrast, the rate of change of the orbital period due to gravitational radiation in this small system is expected to be $\dot{P}_B / P_B \sim 6.10^{-9}$ yr^{-1} (Press and Thorne, 1972) and would be detectable in $\sim$ 50 years.

The sensitivity of the phase measurements at 130 mHz, ϕ_e, cannot be improved beyond the level achieved in this paper because of the non-Poissonian noise contamination from the flickering. The possibility of the flickering occuring in one color band and the pulsations in the other color band is remote (cf, the colors of the 1.24s Feature 1 pulsations from HZ Her, Nelson, Chanan and Middleditch, 1977; the colors of the 71s pulsations in DQ Her, Chanan, Nelson and Margon, 1978; and the colors of the 28s pulsations in WZ Sge, Middleditch, Nelson and Chanan, 1978). On the other hand, the measurement of the $3F_o - 3F_B$ component of pulsation near 390 mHz from the companion star is still statistics limited and is likely to remain that way for the next order of magnitude improvement in light gathering power. Better statistics at $3F_o - 3F_B$ would improve the sensitivity of the measurements of $\underline{a}_c$ sini, ϕ_B and $\underline{a}$ and consequently the masses of the two components. Furthermore, the resulting improved limits or measurements for the periodic amplitude modulation of the $3F_o - 3F_B$ component of pulsation would help to

discriminate between models of pulsed reprocessing in the companion's atmosphere and to estimate the size of the shadow of the disk, reducing the systematic uncertainty in the measurement of $\underline{a}$ in consequence.

Improvement in the measurements via increased photomultiplier quantum efficiency for a blue object such as 4U1626-67 is unlikely. CCD detectors will lose more sensitivity to the readout noise in the time series than they will gain in quantum efficiency. Therefore, significant progress in our understanding of the 4U1626-67 system (and probably all binary X-ray pulsars, systems with accreting material and accretion disks) will require a study similar to that carried out here, but with a Next Generation Telescope (NGT) of aperture 10m or larger in the Southern Hemisphere.

The net measurement error for $\underline{a}_c \sin i$ is $\pm$ 0.08 lt·s, corresponding to 27.2 magnitudes of light. This is obtained from sidelobes of the 3rd harmonic of the companion pulsations at the respective frequencies of $(3F_o - 3F_B) \pm F_B$, $3F_o - 3F_B$ and $F_o - F_B$ and with magnitudes of 25.7, 25.0 and 24.5, whereas the direct pulsations at F_o have a magnitude of 22.65. Since these measurements were made in a system with 18.6 magnitudes of light which flickers and must be observed with a sky background so that the resulting effective background light level at 130 mHz is never less than 16.6 magnitudes of light on the darkest of nights at CTIO, it is not unreasonable to consider the usefulness of a southern NGT.

Our current knowledge of the X-ray beam pattern of 4U1626-67 is more complete than any other known X-ray binary system: The low, medium and high energy X-ray pulse profiles are known in the direction

to the Earth (Rappaport et al. 1977; Pravdo et al. 1979) and the equatorial low energy X-ray pulse profile is known from the companion pulsations. There is, therefore, hope that this extremely faint optical system will lend understanding to the accretion mechanism that no other X-ray binary can.

Authors' note to the revised version, 28Aug80:

Further observations of 4U1626-67 made by JM in April 1980 with the CTIO 4m telescope indicate the lower sidelobe amplitude can fade to ∿10% of the direct pulsation amplitude for at least two consecutive nights (with no strong 3rd harmonic present). On the 6th night of observations in April, 1980, the relative amplitude of the lower sidelobe returned to a level consistent with the 17% relative level observed in 1979 (although bad weather caused this result to be only marginally significant). Observations in June of 1980 by JN with the 1.5 m telescope indicate that relatively strong sidelobe pulsations may fade in 4 days to the weaker state, although these results all have low statistical significance. Orbital phase analysis in the April and June, 1980, observation intervals indicates that these data sets are both independently consistent with an orbital period of 2485s and inconsistent with 2492s.

If the variation in the relative strength of the lower sidelobe is periodic in nature, then the period would have to be 7-11 days or some suitable alias.

ACKNOWLEDGEMENTS

We would like to thank Dr. Alistair Walker, Dr. John Graham and the entire staff of C.T.I.O. without whose help these observations would not have been possible. We thank Steve Pravdo for his assistance with the HEAO A2 data analysis. This work was supported in part by the Department of Energy and N.S.F. grant AST 78-06873. KOM acknowledges financial support from the Miller Institute for Basic Research and NASA grant No. NAGW-44, and partially supported by the U.S. Department of Energy under Contract W-7405-ENG-48.

APPENDIX

ORBITAL PHASE ANALYSIS FOR THE 4U1626-67 OPTICAL PULSAR

We have defined the effective binary phase at t_o:

$$\phi_e(t_o) \equiv \phi_d(t_o) - \phi_c(t_o) \approx \phi_B(t_o) + \underline{a}F_o/c \quad \text{(cycles)} \qquad \text{A1}$$

where the phases, ϕ_d and ϕ_c, are defined for the complex Fourier amplitudes at the central frequencies of the main and lower side-lower peaks (see Section III b of the text). However, the center of the less significant lower sidelobe peaks scatter around a frequency which is F_B lower than the main peak due to statistical errors, $3/(\pi\sqrt{6P}\cdot T_{run})$ (where P is the power in the lower sidelobe peak; cf MN), neglecting the smaller scattering of the main peaks about the true F_o. Moreover, the ϕ_e's so defined would not be appropriate for use in a cycle-counting phase analysis which used any frequency other than F_B' (the frequency corresponding to the exact separation of the two Fourier peaks) to establish the cycle numbers of the times of $\phi_e = 0$. This is evident if we make a Taylor series expansion of the phase of the complex amplitudes in the neighborhood of the lower sidelobe peak:

$$\phi_c(F_o-F_B) = \phi_c(F_o-F_B') + (F_B'-F_B)\cdot d\phi_c/dF + (F_B'-F_B)^2/2\cdot d^2\phi_c/dF^2 + \ldots \qquad \text{A2}$$

Thus,

$$\phi_e \equiv \phi_d-\phi_c(F_o-F_B') = \phi_d-\phi_c(F_o-F_B) + (F_B'-F_B)\cdot d\phi_c/dF + (F_B'-F_B)^2/2\cdot d^2\phi_c/dF^2 + \ldots \qquad \text{A3}$$

In the frequency neighborhood of the lower sidelobe peak where

the true value, F_o-F_B, must lie, the phase is generally well-represented by the constant and linear terms of the Taylor series expansion. This is because the expectation value for the quadratic term is 0 and its rms jitter in phase due to statistical fluctuations is only $(6/5)^{\frac{1}{2}}P^{-3/2}$ radians as compared with the $(3/(2P))^{\frac{1}{2}}$ rms jitter in the linear term due to the same fluctuations (e.g., Middleditch, 1980, unpublished work).

Small changes in F_o, while keeping the peak separation constant, do not affect the values of ϕ_e to first order since the linear drift term in Equation A3, $(F_B^{'} - F_B)\cdot d\phi_c/dF$, cancels a similar term in the expansion for ϕ_d (which is not shown). The problem arises when the phases are derived from points in the continuous Fourier spectrum separated by a varying trial frequency. In this case the ϕ_e's all change due to the $d\phi_c/dF$ terms and runs with different total times will change by differing amounts due to different values of $d\phi_c/dF$ (for steady pulsation the phase drift rate, $d\phi_c/dF$, of the corresponding Fourier peak will scatter about $-T_{run}/2$ with an error of $T_{run}/(2\sqrt{6P})$ (ibid)).

This effect was eliminated by shifting the time for which the ϕ_e's are defined by the corresponding value, $-d\phi_c/dF$, obtained from each run. The ϕ_e values are increased by multiplying $-d\phi_c/dF$ by the empirical value, F_B', determined from the position of the lower sidelobe peak to give, to first order:

$$\phi_e(t = t_o - d\phi_c/dF) = \phi_d(F_o,t_o) - \phi_c(F_o-F_B',t_o) - F_B'd\phi_c/dF =$$

$$\phi_d(F_o,t_o) - \phi_c(F_o-F_B,t_o) - F_Bd\phi_c/dF \qquad \text{A4}$$

The second part of Equation A4 is independent of F_B (to first order) while the last part of the equation is independent of F_B'. We have thus constructed a phase which does not depend on a choice of a particular frequency in its measurement. For convenience, the time of $\phi_e = 0$ nearest to $t_o - d\phi_c/dF$ is chosen to represent the phase point. These times were corrected to the solar system barycenter (for the direction to 4U1626-67) and are listed with their uncertainties in Table 2.

To determine the orbital frequency, F_B, more precisely, trial frequencies were used to fix the number of integral cycles in the time intervals between the separate times of $\phi_e = 0$. The chi-squares for the best straight - line fits in the phase-time plane were calculated for all cycle number assignments corresponding to a ±0.02 mHz range (±1.81 cycles/day) of trial frequencies centered about the 0.4011 mHz average of the five F_B' values from the individual runs (which are also listed in Table 2). The chi-squares of these individual frequencies were also calculated wrt the best fit frequency.

Acceptable fits were found for only two discrete values of the binary period. These are 2492.32s and 2491.05s ± 0.13s which had X^2 values of 1.24 and 3.44 respectively, for 3 degrees of freedom. The next most probable orbital period is 2485.17s which produces a X^2 value greater than 9 for 3 degrees of freedom. Moreover, no possible connections of phase immediately outside of the range from 0.400 to 0.403 mHz have X^2 values less than 10 for 3 degrees of freedom until the trial orbital frequency has changed by nearly 1 cycle per day, 0.116 mHz, and these are definitely excluded by the orbital frequencies measured for the individual runs.

Section III b of the text describes how the orbital period can be determined to a high degree of accuracy even without the exhaustive X^2 analysis. It is therefore possible to check the analysis for the effects of neglecting the higher terms of the dependence of the phase on the frequency near the lower sidelobe peak. Accordingly, the phases of the Fourier amplitudes were measured at exactly 1/2490.5 s lower than the main peaks to determine new time of $\phi_e = 0$ near the start of the runs, t_o. An analysis of trial cycle counting for the new $\phi_e = 0$ times gives results that are virtually identical to those obtained from the analysis of the times near the centers of the runs, with 2492,33s and 2491.06s ± 0.13s as the only possible binary orbital periods consistent with the data. The next most likely orbital period was still 2485.2s and had an a priori probability of less than 5% for its X^2 value near 9.

REFERENCES

Abramowitz, M. and Stegun, I. A. 1970, "Handbook of Mathematical Functions", National Bureau of Standards Applied Mathematics Series , 55, Ninth Printing, L.C.C.C. No. 64-60036, P. 360.

Bradt, H. V., Doxey, R. E. and Jernigan, J. G., Proceedings of the COSPAR/IAU Symposium, Innsbruck, in X-ray Astronomy, Ed. Baity and Peterson, Pergamon Press, 1979, Page 3.

Chanan, G. A., Nelson, J. E. and Margon, B. 1978, Ap. J., 226, 963.

Chanan, G. A., Middleditch, J. and Nelson, J. E. 1976, Ap. J., 208, 512.

Chanan, G. A. 1978, Ph. D. Thesis, LBL Report No. 7227.

Chester, T. 1979, Ap. J., 227, 569.

Chester, T. 1977, Ph. D. Thesis, Princeton University.

Gruber, R., Koo, D. and Middleditch J. 1980, preprint, submitted to PASP.

Ilovaisky, S. A., Motch, Ch. and Chevalier, C. 1978, Astr. Ap., 70, L19.

Ilovaisky, S. A., Chevalier, C. and Motch, Ch. 1980, Talk presented at the High Energy Astrophysics Division Meeting of the AAS, Cambridge, Mass.

Joss, P. C., Avni, Y. and Rappaport, S. 1978, Ap. J., 221, 645.

Li, F. K., Joss, P. C., McClintock, J. E., Rappaport, S. and Wright, E. L. 1979, preprint, submitted to the Astrophysical Journal.

Lubow, S. H. and Shu, F. H. 1975, Ap. J., 198, 383.

Lubow, S. H. and Shu, F. H. 1976, Ap. J., (Letters), 207, L53.

McClintock, J. E., Canizares, C. R., Bradt, H. V., Doxsey, R. E., Jernigan, J. G. and Hiltner, W. A. 1977, Nature, 270, 320.

McClintock, J. E., Canizares, C. R., Li, F. K. and Grindlay, J. E. 1980, Ap. J. (Letters), 235, L81.

Middleditch, J. 1976, Ph. D. Thesis, LBL Report No. 3639.

Middleditch, J. and Nelson, J. 1976, Ap. J., 208, 567.

Middleditch, J., Mason, K., Nelson, J. and White, N. 1979, IAU Circ. No. 3364.

Middleditch, J., Nelson, J. and Chanan, G. A. 1979. Talk presented at the 151st Meeting of the AAS, abstract published in the BAAS, 9, No. 4, part 11.

Nelson, J., Chanan, G. A., and Middleditch, J. 1977, Ap. J., 212, 215.

Peterson, B. A., Wallace, P., Elliott, K. H., Hill, P. W. and Manchester, R. N. 1980, M. N. R. A. S., 190, 33p.

Pravdo, S. H., White, N. E., Boldt, E. A., Holt, S. S., Serlemitsos, P. J., Swank, J. H., Szymkowiak, A. E., Tuohy, I. and Garmire, G. 1979, Ap. J., 231, 912.

Press, W. H. and Thorne, K. S. 1972, Ann. Rev. A. A., 10, 343.

Pringle, J. E. 1975, M. N. R. A. S., 170, 633.

Rappaport, S. Markert, T., Li, F.K., Clark, G.W., Jernigan, J.G. and McClintock, J.E. 1977, Ap.J. (Letters), 217, L29.

Roemer, O. and Scavens, J. 1976, reprinted in Isis, 31, P. 233, (7Dec76).

TABLE 1: JOURNAL OF OBSERVATIONS

RUN	UT DATE	START JD-2,440,000.5 Local Time	DURATION Hrs	TELESCOPE	APERTURE "	CONDITIONS
1	24Apr79	3987.10808	5.2	4-m	9.6	some clouds
2	24Apr79	3987.32862	1.8	4-m	6.3	clear
3	25Apr79	3988.18264	1.5	4-m	6.3	clouds
4	25Apr79	3988.24576	0.2	4-m	6.3	rain!
5	26Apr79	3989.11576	6.7	4-m	6.3	Photometric
6	19Jun79	4043.22014	1.9	1.5-m	4.8	Photometric
7	21Jun79	4045.20486	1.8	1.5-m	6.6	some clouds
8	23Jun79	4047.06043	1.9	4-m	6.3	some clouds
9	23Jun79	4047.97292	2.9	4-m	5.1	Photometric
10	24Jun79	4048.09723	6.4	4-m	6.3	deteriorated seeing
11	25Jun79	4049.06008	4.75	4-m	6.3	Photometric
12	25Jun79	4049.26706	1.0	4-m	6.3	Photometric
13	14Aug79	4099.03543	4.2	4-m	6.3	End Clouds
14	18Aug79	4103.04413	4.0	1.5-m	6.2	Photometric
15	21Aug79	4106.04949	0.7	1.5-m	6.2	Photometric
16	21Aug79	4106.13913	1.7	1.5-m	6.2	Photometric

TABLE 2: 2492-SECOND ORBITAL PHASING

RUN	TIME OF $\phi_e = 0$ JD-2,440,000.5	UNCERTAINTY sec	ORBITAL FREQUENCY milliHertz	2492.33s PHASE Cycles	2491.06s PHASE Cycles
1+2	3987.28856	162	0.3987 (.0068)	-2111	-2112
5	3989.27701	125	0.4093 (.0079)	-2042	-2043
9+10	4048.18162	63	0.4028 (.0028)	0	0
11+12	4049.16200	78	0.3925 (.0047)	34	34
13	4099.12472	140	0.4184 (.0138)	1766	1767

TABLE 3

RESULTS FROM PHASE AND AMPLITUDE MODULATION FOR 4U1626-67 AT $3F_o - 3F_B$

RUN	$\underline{a}_c \sin i$ lt·s	ϕ_e	$\phi_{B_{eff}}^*$	$\Delta\phi$	z_A 90%	ϕ_f
1+2	----	307°	237°	$70^\circ(50^\circ)$	---	-53° (24°)
5	$0.34^{+0.13}_{-0.09}$	190°	159°	$31^\circ(27^\circ)$	< 0.57	$-8.4^\circ(18^\circ)$
9+10	$0.47^{+0.22}_{-0.19}$	327°	245°	$82^\circ(30^\circ)$	< 0.62	-30° (12°)
11+12	$0.16^{+0.17}_{-0.16}$	219°	240°	$-21^\circ(35^\circ)$	< 1.0	$-8.5^\circ(16^\circ)$
13	$0.34^{+0.18}_{-0.18}$	348°	270°	$78^\circ(40^\circ)$	< 0.95	$-16.5^\circ(24^\circ)$
	$0.32^{+0.08}_{-0.07}$			$46.4^\circ(15^\circ)$	< 0.48	-22° (7.6°)

$\underline{a}$ = $(46.4/360^\circ)$ cycles x 7.68 s/cycle = 0.99 (32) lt·s.

*This is ϕ_B as discussed in Section III d and $\phi_{B_{eff}}$ as discussed in Section III f when a new systematic effect is discovered by the model calculations.

TABLE 4

4U1626-67 OPTICAL PULSE PROFILES

Profile (F) = $\alpha_1\cos(2\pi Ft) + \alpha_2\cos2(2\pi Ft+\phi_2) + \alpha_3\cos3(2\pi Ft+\phi_3)$ where $\alpha_n \equiv \alpha(nF)/\alpha(F_o)$; $F_o = 0.13025$ Hz

RUN	FREQUENCY	PULSED FRACTION %	α_1	α_2	ϕ_2	α_3	ϕ_3
1+2	F_o	2	1.000	0.357(.053)	$-90.^{o}4$ ($5.^{o}3$)	0.140(.052)	$-1^{o}(7^{o})$
	F_o-F_B	0.26(.12)	0.13(.06)	0.123 "	$+64^{o}$ (24^{o})	0.103 "	$+53^{o}(23^{o})$
5	F_o	2.4(.4*)	1.000	0.291(.033)	$-87.^{o}5$ ($3.^{o}8$)	0.087(.032)	$-3^{o}(6^{o})$
	F_o-F_B	0.29(.12)	0.12(.05)	0.077 "	$+26^{o}$ (19^{o})	0.147 "	$+5^{o}(17^{o})$
9+10	F_o	2.1(.4*)	1.000	0.247(.033)	-101^{o} ($4.^{o}$)	0.090 "	$+10^{o}(5.^{o}4)$
	F_o-F_B	0.49(.08)	0.23(.04)	0. "	$+34^{o}$ (33^{o})	0.069 "	$+40^{o}(11^{o})$
11+12	F_o	2.5(.4*)	1.000	0.302 "	-93^{o} ($3.^{o}3$)	0.064 "	$+6^{o}(7^{o})$
	F_o-F_B	0.47(.10)	0.19(.04)	0.061 "	$+38^{o}$ (15^{o})	0.115 "	$+15^{o}(12^{o})$
13	F_o	2.8(.4*)	1.000	0.34(.050)	$-87.^{o}8$ ($5.^{o}3$)	0.055(.043)	$+19^{o}(11^{o})$
	F_o-F_B	0.43(.21)	0.154(.075)	0.006 "	$+34^{o}$ (25^{o})	0.146 "	$+35^{o}(21^{o})$
	F_o	2.45	1.000	0.295(.017)	$-92.^{o}5$ ($1.^{o}8$)	0.083(.016)	$+5.^{o}6(3.^{o}4)$
		Absolute:	2.45%	0.72%		0.20%	
	F_o-F_B	0.42	0.18(.02)	0.056 "	$+38^{o}$ (9^{o})	0.115 "	$+27.^{o}4(6.^{o}5)$
		Absolute:	0.42%	0.14%		0.28%	
		Corrected for Orbit:		0.15%		0.33%	
Used for fit by Peterson et al, (1980):	F_o		1.000	0.352	$-80.^{o}2$	0.163	$+3.^{o}8$
This work:	F_o		1.000	0.295(.017)	$-92.^{o}5(1.^{o}8)$	0.083(.016)	$+5.^{o}6(3.^{o}4)$
" " :	F_o-F_B	(relative)	1.000	0.35 (.08)	$+38^{o}$ (9^{o})	0.79 (.11)	$+27.^{o}4(6.^{o}5)$

* The uncertainty of the absolute amplitude scale is limited by systematic effects of background and transparency which do not effect any of the relative amplitude measurements.

TABLE 5

Model Systematic Corrections for 4U1626-67

MODEL NUMBER	ORBITAL INCLINATION i	DISK SHADOW THICKNESS+	MASS RATIO R	ILLUMINATED ROCHE LOBE $\Omega_{RL}/4\pi$* %	ORBITAL PHASE CORRECTION $\phi_{Beff}-\phi_{B}$	CORRECTION FACTOR FOR $\frac{a_1 \sin i}{z_{\phi}/z_{\phi eff}}$	CORRECTION FACTOR FOR $\frac{a}{a/a_{eff}}$	AMPLITUDE MODULATION FRACTION ++	MINIMUM pf_x REQUIRED %
1	22.°5	--	0.1	0.389	-13.°6	1.405	1.229	0.584	.42
"	"	0.05	"	0.309	-10.2	1.339	1.253	0.474	6.3
"	"	0.075	"	0.251(288)	- 5.9	1.294	1.256	0.422	11.4
"	25°	"	"	0.241	- 6.1	1.317	1.234	0.491	
"	22.5	0.10	"	0.197	- 4.5	1.269	1.270	0.379	19.0
"	"	--	0.05	0.256	- 8.3	1.326	1.151	0.584	.42
Chester	"	"	"	---	- 9.0	1.193	1.153	0.427	.42
1	"	0.05	"	0.186	- 4.4	1.240	1.173	0.445	11.7
"	"	0.075	"	0.145	- 4.1	1.211	1.190	0.390	22.
"	"	--	0.02	0.145	- 6.2	1.260	1.081	0.580	.42
"	"	0.025	"	0.123	- 4.1	1.213	1.101	0.489	9.0
"	"	0.05	"	0.088	- 1.9	1.160	1.102	0.400	24.2
"	"	--	0.01	0.093	- 4.9	1.224	1.045	0.575	.42
"	"	0.02	"	0.079	- 3.2	1.177	1.063	0.483	11.1
"	"	0.04	"	0.057	- 1.4	1.133	1.067	0.393	29.6
2	"	--	0.1	0.393(461)	- 7.4	1.241	1.274	0.244	.42
"	"	0.05	"	0.266	- 1.6	1.213	1.328	0.044	8.3
"	15.°	"	"	0.286	- 0.1	1.238	1.338	0.015	7.8
"	30.	"	"	0.241	- 3.6	1.213	1.282	0.167	9.1
"	22.5	0.075	"	0.200(232)	- 0.1	1.218	1.333	0.020	16.2
"	"	0.10	"	0.146	- 0.3	1.205	1.346	0.016	29.2
"	"	--	0.05	0.256	- 6.0	1.200	1.195	0.268	.42
"	"	0.05	"	0.150	+ 0.3	1.165	1.247	0.015	14.4
"	"	0.075	"	0.109	- 0.4	1.149	1.266	0.012	29.3
"	"	--	0.02	0.142	- 4.3	1.139	1.126	0.280	.42
"	"	0.025	"	0.107	- 1.5	1.131	1.170	0.162	10.2
"	"	0.05	"	0.066	+ 0.6	1.106	1.166	0.008	31.8
"	"	--	0.01	0.091	- 4.3	1.112	1.089	0.277	.42
"	"	0.02	"	0.068	- 1.2	1.101	1.129	0.160	12.4
"	"	0.04	"	0.042	+ 0.5	1.080	1.129	0.005	40.

+ This gives the half width of the disk shadow about the equator or equivalently, the fraction of solid angle that the disk subtends at the X-ray source.

* This is the mean effective solid angle fraction subtended by the X-ray illuminated part of the companion's Roche lobe at the X-ray source and visible to the Earth.

++ This is the mean semi-amplitude of the amplitude modulation of the 3rd harmonic of the optical pulsations from the companion due to the orbital motion.

AUTHORS ADDRESSES

K.O. Mason
Space Sciences Laboratory
University of California
Berkeley, CA 94720

J. Middleditch
MS 436
Los Alamos Scientific Lab
P.O. Box 1663
Los Alamos, NM 87545

J.E. Nelson
Bldg #50
Lawrence Berkeley Laboratory
University of California
Berkeley, CA 94702

N.E. White
Code 661
Goddard Space Flight Center
Greenbelt, MD 20771

FIGURE LEGENDS

Fig. 1. The broadband optical intensity of 4U1626-67 Run 11 + 12 vs. time for a 6 hr interval taken on the 4m telescope on 25Jun79 UT. The relative orbital phase (ϕ_e -- see text) is plotted on the lower horizontal axis for reference. The data between cycles 6 and 7.5 have been edited for this Figure since poor guiding affected the quality of the light curve.

Fig. 2. Detailed sections of Fourier power vs. frequency for Runs 5, 9 + 10, and 11 + 12 near the nominal X-ray pulsation frequency of 130.26 mHz. The peaks due to the direct optical pulsations at the same frequency all rise above 300 and had to be truncated in the Figure. The $(\sin y/y)^2$ ($y \equiv \pi[F-F_o]\cdot T_{run}$) sidelobes symmetric about (and due to) the high peaks have been mathematically suppressed when these continous Fourier spectra were generated by interpolation using the discrete Fourier amplitudes. The persistent lower sidelobe which occurs at 129.86 mHz is identified with optical pulsations from the binary companion of the X-ray source produced via X-ray to optical reprocessing.

Fig. 3. The orbital geometry of the 4U1626-67 binary system with $R = M_C/M_X = 0.05$, an inclination $i = 22.^{\circ}5$ and with an orientation corresponding to orbital phase, $\phi_B = 180^{\circ}$. The projected orbital radii for the Roche filling companion

star and the X-ray pulsar, $\underline{a}_C \sin i$ and $\underline{a}_X \sin i$, are shown along with the total orbital separation, $\underline{a}$.

Fig. 4. (a) A detail of the Fourier power spectrum of Run 5 near $3F_o - 3F_B$ -- the 3rd harmonic frequency of the companion pulsations. The power at this frequency is highly significant (the probability of it exceeding some P_o is e^{-P_o}) and larger than the power at $3F_o$ corresponding to the third harmonic of the direct pulsations.

(b) The power spectrum for the phase modulation of Run 5 defined as half the squared modulus of the sum of the Fourier amplitudes a_+ and a_- from Equation 6 (see text). The upper horizontal scale defines ΔF -- the frequency of the modulation. A significant modulation is indicated for $\Delta F = 1$ cycle/2492s orbit. One other source of modulation near $\Delta F = 0.3$ cycles/2492s orbit which arises from the two sidelobes close to the peak at $3F_o - 3F_B$ is not understood but does not affect the $\Delta F = 1$ measurement and does not persist in the other runs.

(c) The power spectrum for the amplitude modulation of Run 5 as defined from Equation 7 in the text. No amplitude modulation is found near $\Delta F = 1$ cycle/2492s orbit. The non-persistent sidelobes near $3F_o - 3F_B$ produce an apparent amplitude modulation at 0.2 cycles/2492s orbit but do not affect the measurement synchronous with the orbital period (at $\Delta F = 1$ cycle/2492s orbit).

Fig. 5. The pulse profiles for the direct and companion pulsations for Run 5 produced by folding the data at the frequencies F_o and $F_o - F_B$ are plotted as pulsed fraction against the 7.68s pulse phase. The two profiles have been aligned so that the two Fourier components at their fundamental frequencies agree in phase. The mean effective projected orbit derived for the companion star ($\underline{a}_c \sin i = 0.32$ lt·s) has been used to fold the data at $F_o - F_B$. The consequences of the dissimilarities of the two pulse profiles are discussed in Section V.

Fig. 6. The companion's Roche geometry for the 4U1626-67 orbital system with R = 0.05, i = 22°.5 and a total orbital separation of 1.000 lt·s. The boundary of X-ray illumination on the companion's surface is plotted as a dashed "curve" (the projections onto two of the three orthogonal planes are almost straight lines) while the boundaries of visibility of the surface at the Earth are plotted as dots with hourglass, square, or diamond markers for orbital phases 0^o, 90^o, and 180^o respectively. The path from the X-ray source to the companion is inclined by 3^o to the orbital plane -- just outside a ±0.05 radian equatorial shadow.

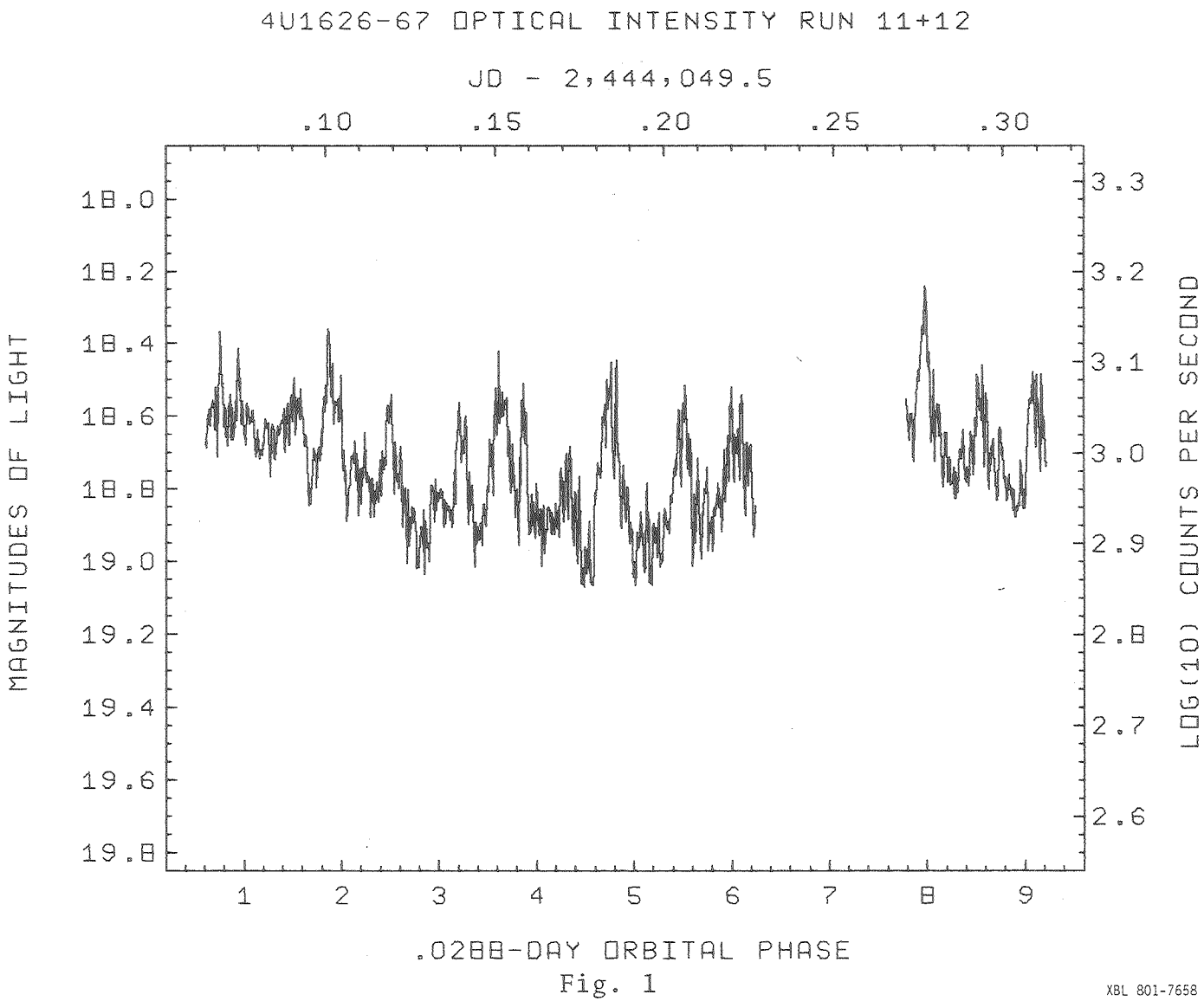

Fig. 1

XBL 801-7658

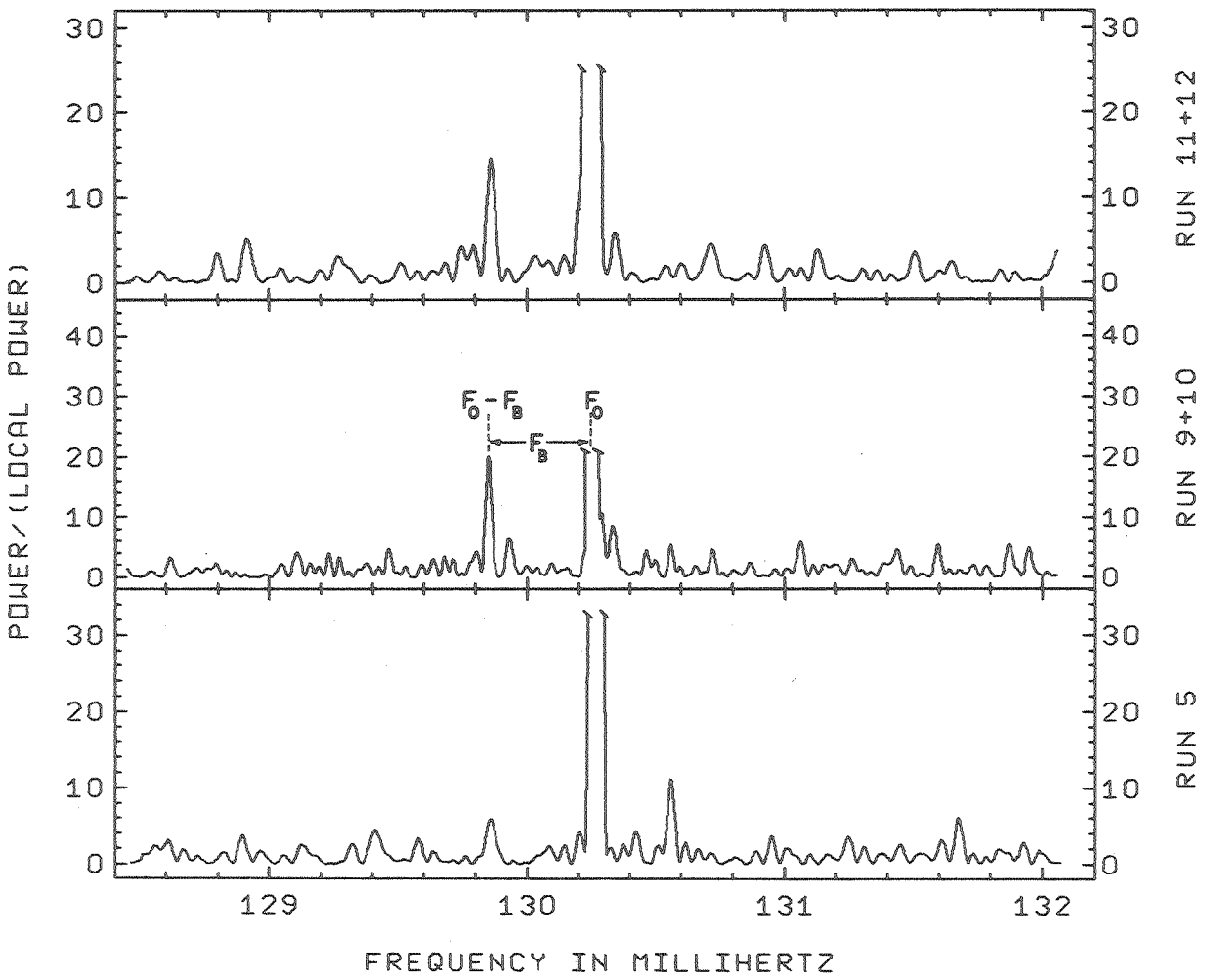

Fig. 2

XBL 801-7659

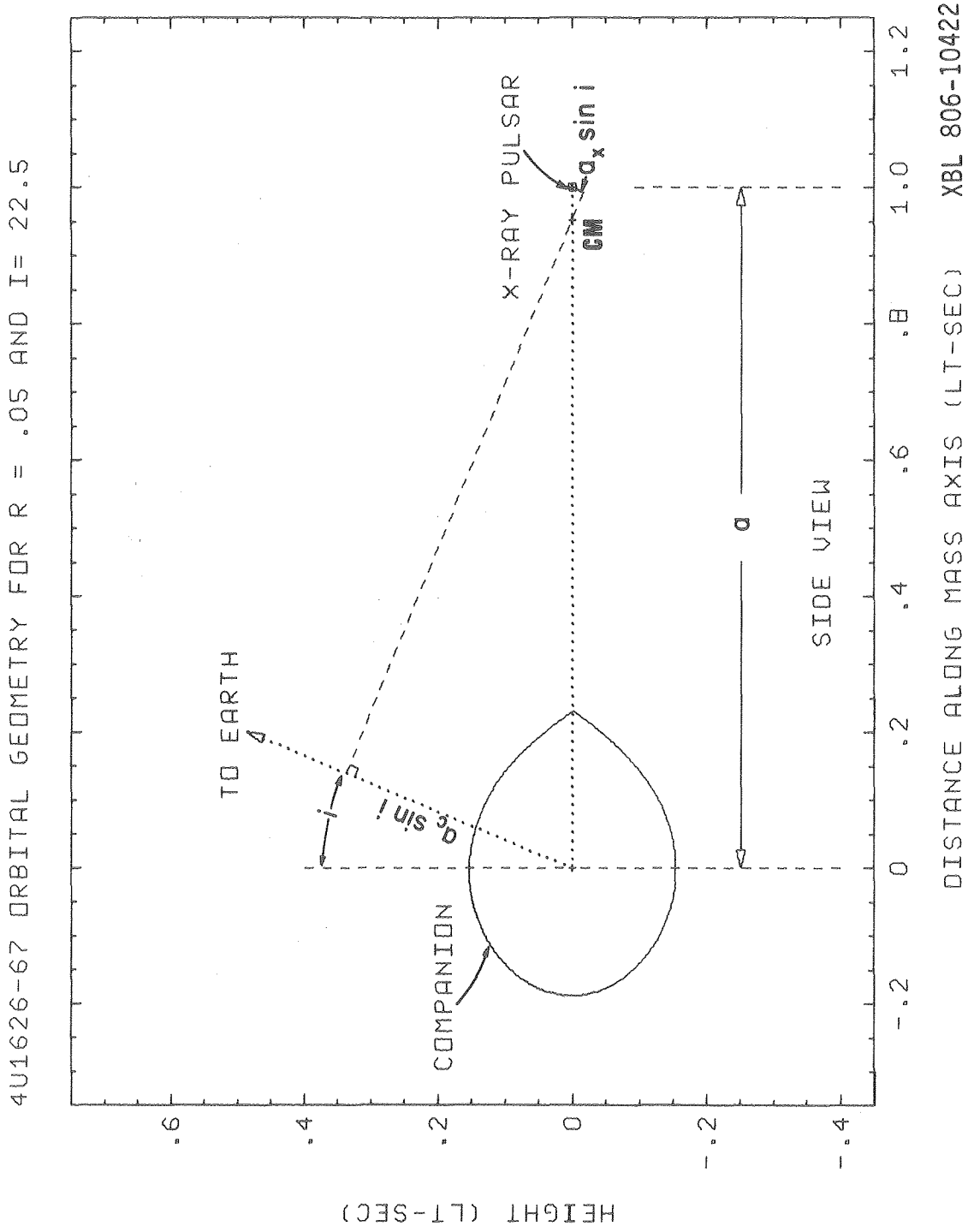
4U1626-67 ORBITAL GEOMETRY FOR R = .05 AND I= 22.5
HEIGHT (LT-SEC)
.6
.4
.2
0
-.2
-.4
-.2
0
.2
.4
.6
.8
1.0
1.2
DISTANCE ALONG MASS AXIS (LT-SEC)
X-RAY PULSAR
CM
$a_x \sin i$
TO EARTH
$a_c \sin i$
i
COMPANION
SIDE VIEW
a
XBL 806-10422

Fig. 3

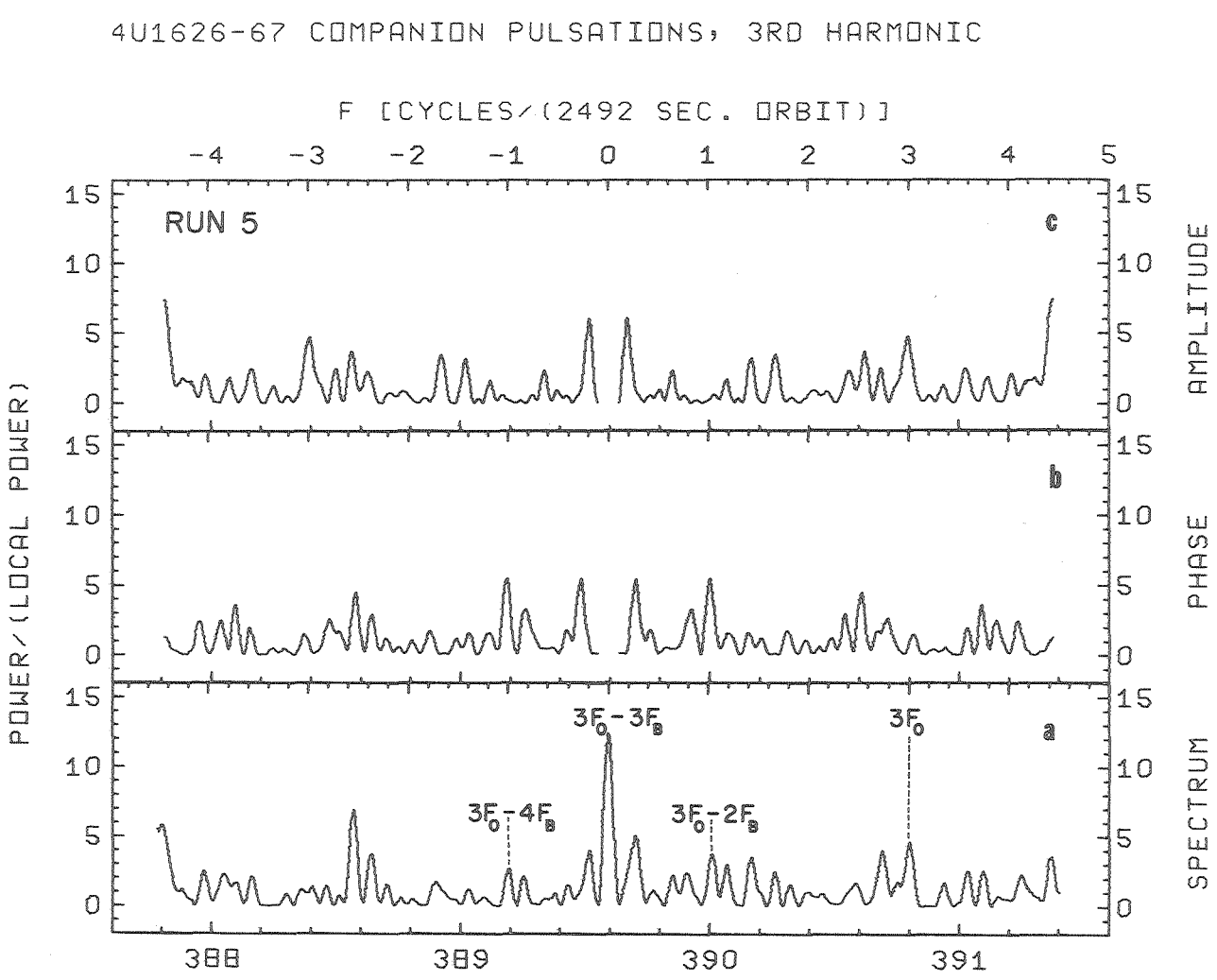

Fig. 4

XBL 801-7652

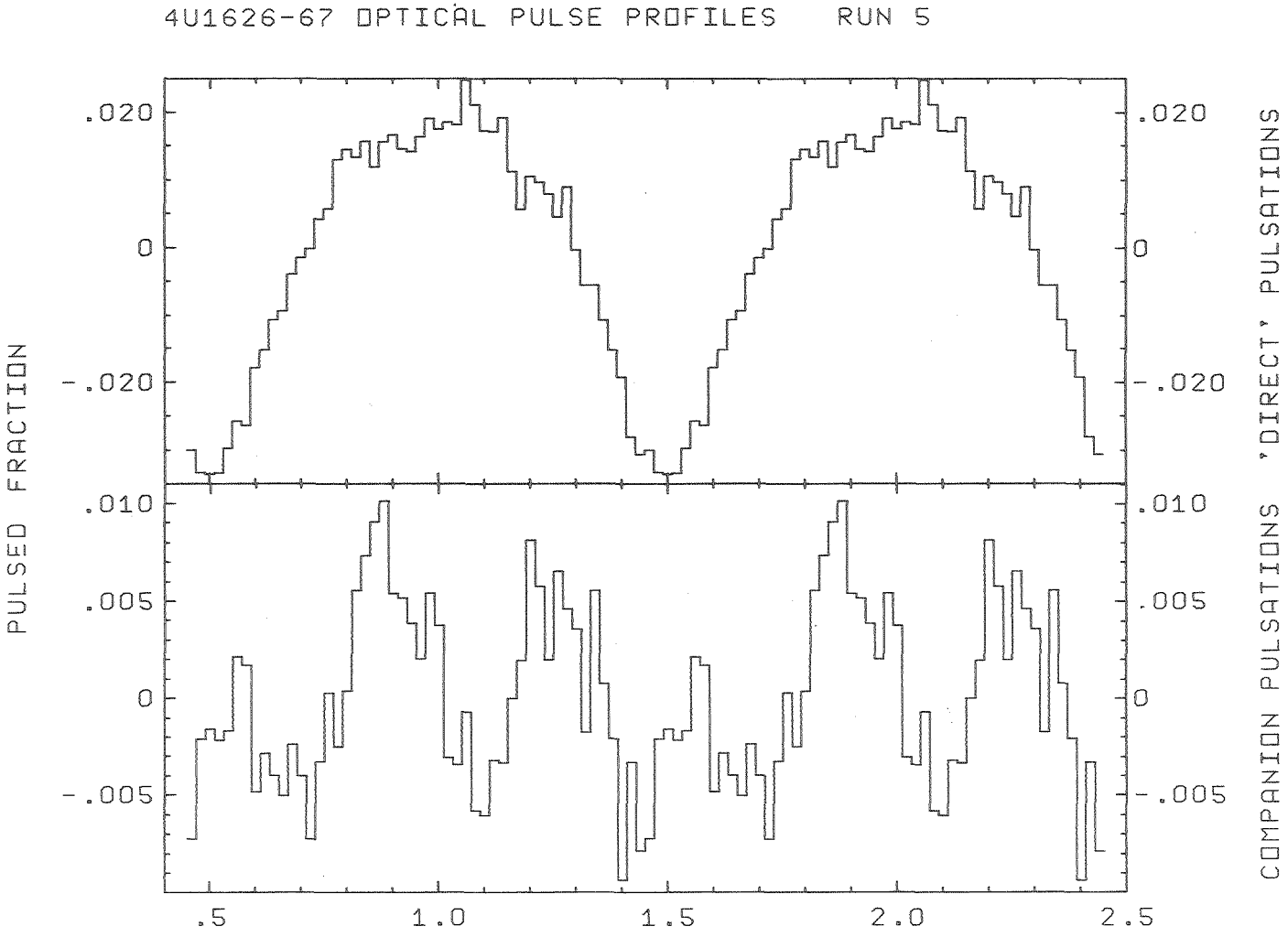

Fig. 5

XBL 803-8795

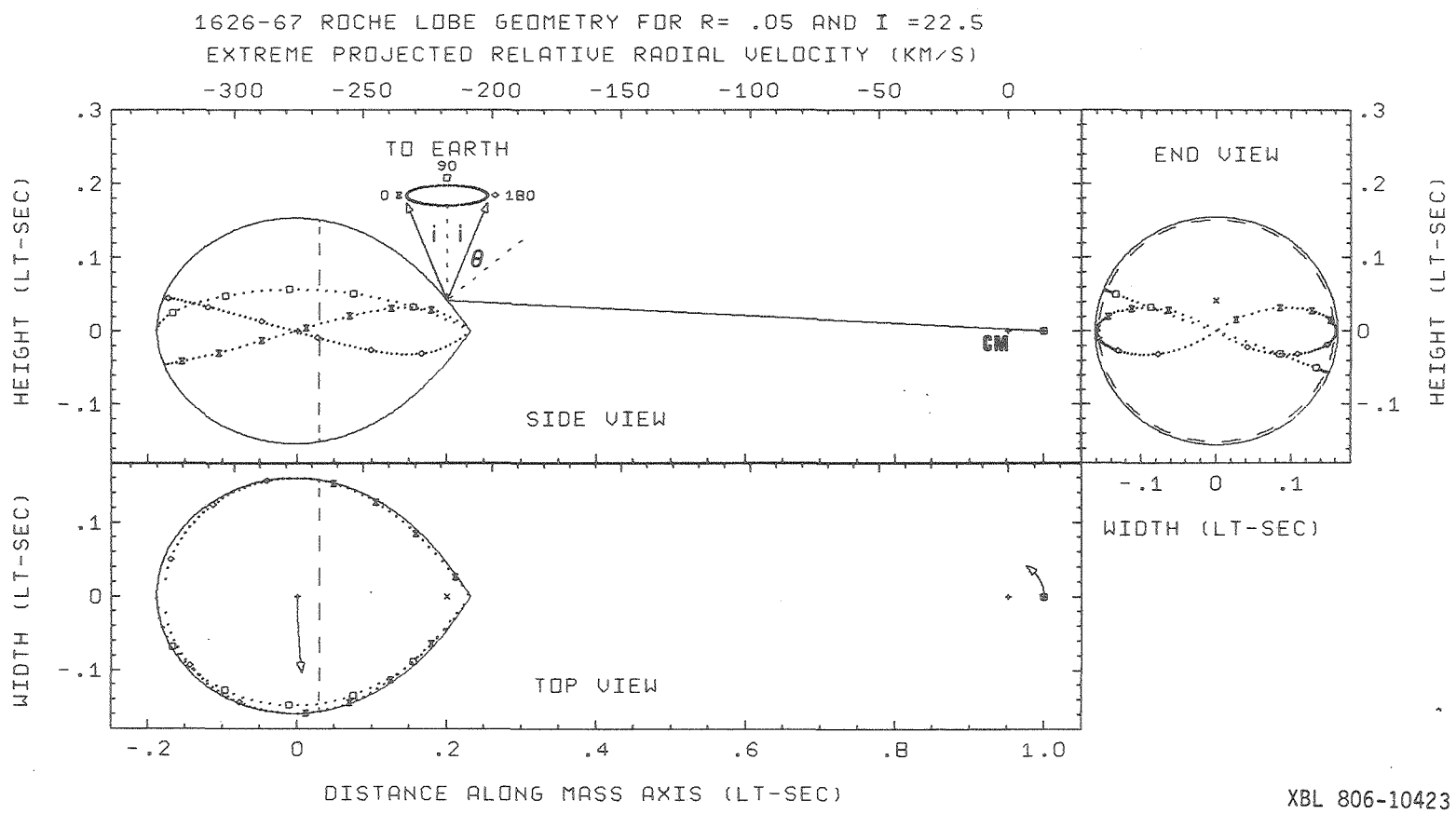
1626-67 ROCHE LOBE GEOMETRY FOR R= .05 AND I =22.5
EXTREME PROJECTED RELATIVE RADIAL VELOCITY (KM/S)
-300
-250
-200
-150
-100
-50
0
TO EARTH
90
0
180
θ
i
CM
SIDE VIEW
END VIEW
TOP VIEW
HEIGHT (LT-SEC)
WIDTH (LT-SEC)
.3
.2
.1
0
-.1
-.2
.4
.6
.8
1.0
DISTANCE ALONG MASS AXIS (LT-SEC)
XBL 806-10423

Fig. 6